2009-01-01

Effect Of Air Addition On Plasma-Based Reforming Of Methane And Propane

Atul Vitthalrao Ambhore
University of Texas at El Paso, atulambhore25@gmail.com

EFFECT OF AIR ADDITION ON PLASMA–BASED REFORMING OF METHANE AND PROPANE

ATUL VITTHALRAO AMBHORE, B.E.

Department of Mechanical Engineering

APPROVED:

_____
Evgeny Shafirovich, Ph.D., Chair

_____
Ahsan Choudhuri, Ph.D.

_____
Felicia Manciu, Ph.D.

_____
Patricia D. Witherspoon, Ph.D.
Dean of the Graduate School

This thesis is dedicated to my family

EFFECT OF AIR ADDITION ON THE PLASMA–BASED REFORMING OF METHANE AND PROPANE

By

ATUL VITTHALRAO AMBHORE

THESIS
Presented to the Faculty of the Graduate School of
The University of Texas at El Paso
in Partial Fulfillment
of the Requirements
for the Degree of

MASTER OF SCIENCE

Department of Mechanical Engineering
THE UNIVERSITY OF TEXAS AT EL PASO
December 2009

ACKNOWLEDGMENTS

I would like to sincerely thank my advisor Dr. Evgeny Shafirovich for his guidance and assistance in my thesis. I would also like to thank my other committee members Dr. Ahsan Choudhuri and Dr. Felicia Manciu for their support and valuable input.

I would like to thank Dr. Kim for his profound supervision, valuable suggestions and constructive feedback which guided me throughout my experiments for my thesis. I would also like to thank all the EAFRL lab members, for their assistance during the course of this research. Special thanks to Dr. Ahsan Choudhuri for giving me financial support and allowing me to use the combustion lab to conduct my experiments.

I sincerely thank Mahesh Tonde, Amit Lopes, Asim Inamdar and Yeshi Tenzin. for their friendship and companionship, for all their help (on this research and beyond), for the enjoyable conversations, delicious meals, and great time spent together.

My deepest and most sincere gratitude goes to my family, the constant in my life, especially my parents: Vitthalrao Ambhore and Suman Ambhore, my brother Rahul, and my sister Ashwini, for all the support and love they have always given me. Thanks for listening to me through the good and bad times and for always being there for me.

This thesis was submitted to the supervising committee on December 7, 2009.

TABLE OF CONTENTS

LIST OF TABLES

LIST OF FIGURES

Chapter 1 INTRODUCTION

Combustion plays an important role in modern life. It is a major source of energy. Heat and work, to get these, we burn fuel and oxidant; this is the key to the mankind existence. Combustion includes different processes like thermal, hydrodynamic and chemical. The output of combustion processes can be mechanical work (automobiles and aircraft), heat (boiler, furnaces), light, chemical products and, unfortunately, pollution. In the recent years, the effect of the increasing number of vehicles on the global environment (air pollution) has attracted more attention. Therefore**,** it is essential to maximize the efficiency of varied combustion processes to conserve fuel and reduce pollution. For instance, it is a current demand to have clean and high energy fuel for the combustion in motor vehicles and machinery. Being concerned about the stringent regulations to reduce the pollution and the demand for low cost and high efficiency fuel, many researchers have focused their attention to new emerging technologies which may improve the combustion processes. Plasma-assisted combustion is one of these technologies.

The use of plasmas in various industries has increased in recent years. Plasma processes are used widely in the electronics industry to dope semiconductors and in microcircuit fabrication to etch and deposit thin films. Plasma processes are now being considered in air purification systems to remove trace contaminants by converting them to less harmful species via reactions in a plasma reactor. It is proved that by applying electric field on the flame, one can affect its propagation velocity and stability. There are many ways to allow combustible gas mixtures to operate outside their flammability limits, such as external electrode, arc discharges, plasma jet and corona discharges. It is

well known that all combustion processes depend on the breakdown of the fuel into reactive species and free radicals, which initiates the combustion. Typically the breakdown is achieved using spark ignition, where a high voltage spark discharge (thermal plasma) creates the requisite free radical or ion reactive species, so reaction with oxygen can occur. Burning then continues by the propagation of reactive species generated by the heat of reaction. Thus the efficiency of generation of the new reactive species in spreading flame usually determines the overall combustion reaction rate. The faster the reaction rate, the higher the temperature of combustion process, with detonations producing the highest temperatures and faster pressure rise [82].

Besides that, atmospheric pressure non-thermal plasma has various uses in environmental, biological, and other applications such as expanding the lean combustion in the engine and reducing the soot formation and eliminating CO and NO to non measurable level. That is why plasma is currently receiving lot of attention from alternate fuel researchers. Plasma can be generated through different methods, e.g. pulse corona discharges, dc arc discharges, or spark, dielectric barrier discharges, etc. Among these, dielectric barrier discharge is perhaps the most extensively studied atmospheric pressure glow discharge.

Chapter 2 LITERATURE REVIEW

2.1 Introduction to plasma

Plasma is an ionized gas. It is obtained by applying high voltage externally to the gas, which results in electrical breakdown. Plasma considered as the 4^{th} state of matter, and it consists of positive and negative ions, electrons and some neutral species [1]. Plasmas have a wide range of applications in high technology areas, e.g. materials fabrication processes involving etching for micro-electronics and micro-optical components, and deposition of conducting, magnetic, insulating, polymeric and catalytic thin-films. It is also useful for illumination, microwave generation, annihilation of toxic wastes, laser and chemical synthesis [2, 3].

Laboratory made plasma can be divided into two types: thermal (high temperature or fusion plasma) and non-thermal (cold or gas discharge). This division is based on thermodynamic equilibrium inside the plasma. In thermal plasma, ions, electrons, and neutrals species are in thermodynamic equilibrium, i.e. at the same temperature. The temperature can change from few thousand Kelvin for plasma torches to higher than million Kelvin for fusion plasma. In other cases, the electron temperature is very high (ten thousand Kevin to more than 100,000 K) as compared to the temperature of ions and neutral species, which is approximately the same as room temperature (300 K to 2500 K) [1]. Furthermore, electrons are not in equilibrium within their own ensemble. The main cause of this is thermodynamic non-equilibrium between direct and reverse processes. For example, collisions of fast electrons are responsible for gas excitation and production of electron-ion in plasma volume, consequently, radiation getaway to the wall and electron and radiation are lost in plasma. That is why, in gas discharge, the collision rate

is generally very small, high energy electrons are constrained for inelastic collision to bring a large volume of low energy electrons to an equilibrium with high-energy electrons [5]. This thesis emphasizes the study effect of plasma on conversion of methane and propane to higher hydrocarbons and air as a co-reactant.

2.2 Classification and overview of gas discharges

Gas discharges can be classified as follows:

- Self-sustained discharge
- Non-self sustained discharge.

Self-sustained discharges divide into steady and quasi-steady. These discharges contain arc and glow discharge. The Townsend dark discharge is similar to glow discharges and is characterized by small values of current with cold cathode. Corona is also a low-current self-sustaining discharge, with feature of arc discharge and glow discharge [4]. Coronas may be positive or negative. This is determined by the polarity of voltage on highly curved electrode [37]. The non-self sustain discharges, maintained by electron beams are generally used in electric-ionization lasers.

2.2.1 Glow discharge

The glow discharge is the most studied and the universally applied type of gas discharge [4]. The simplest type of glow discharge is the direct-current glow discharge. The gas discharge is formed by applying adequate high potential difference between two electrodes in the gas medium, breaking down into positive ions and electrons, giving rise to a gas discharge. Initially, few electrons are emitted from the cathode because of omnipresent cosmic radiation. These electrons are not able to sustain discharge by their

own (in the absence of external applied voltage). When potential difference is applied, electrons in front of the cathode get accelerated by the electric field and then collide with the gas atoms. In this collision process, the most crucial collision for ionization and excitation is inelastic collision. The excitation collision is followed by de-excitation by the emission of radiation. The ionization collisions create new electron and ions. These ions afterwards drive toward the cathode by an electric field. The cathode then releases new electrons, which is called the ions induced secondary electron emission. Furthermore, these electrons support new ionization collisions, creating new ions and electrons. These processes of electron emissions at the cathode and the ionization are responsible for making glow discharge a self-sustaining one. Due to this characteristic, electrodes play an important role in the glow discharge [23]. When sufficiently high voltage is applied, ions and atoms strike on the cathode, this not only releases secondary electrons but also atoms from cathode material. This phenomenon is called sputtering and it is used in analytical spectrochemistry [23].

The glow discharge is a self-sustaining discharge with a cold cathode which releases electrons because of secondary emissions, usually due to positive ion bombardment [4]. In glow discharge, the potential difference between cathode and anode is not uniform; it drops after few millimeters in front of the cathode [23]. This drop is known as the cathode fall, and the thickness of the cathode fall layer is inversely proportional to the pressure of the gas. An electrically neutral plasma region of weak field is built between the cathode layer and the anode, if distance between electrodes is sufficiently large. Its relatively homogeneous middle part is called a positive column. It is considered as the most common example of weakly ionized non-equilibrium plasma

sustained by an electric field; it is also separated from the anode by an anode layer. In the formation of the glow discharge, the cathode layer plays an important role. If distance between the electrodes is not sufficient to form a cathode layer, then there will not be any ignition of glow discharge [4].

2.2.2 Atmospheric pressure glow discharge (APGD)

Glow discharge can be generated over a wide extensive range of pressures. Glow discharge can be generated at or near to atmospheric pressure by overcoming some technical problems, such as the overheating at the cathode, followed by arching between the electrodes. This technical problem can be overcome by controlling the product of parameters (*pd*), where "*p*" is pressure and "*d*" is the distance between electrodes. Pressure for the gas can be increased at the cost of the characteristic length between electrodes and still keep *pd* constant [23]. Besides, the glow discharge can also be regulated by selecting the electrode structure, type of gas and frequency of applied voltage [46].

Several researchers found that there are three areas in which some discharges are observed at atmospheric pressure. By changing the design parameter different discharges can become atmospheric pressure glow discharge, e.g. partial discharges [6, 7], lasers, and cold plasma processing [9]. It is important to find the feature of discharges called atmospheric pressure glow discharge (APGD). Generally a partial discharge is normally pulse discharge but partial APGD is characterized as a pulseless discharge because the charge is less than 1 pC. It appears as a diffuse glow within the electrode space during a substantial portion of ac half cycle. Similarly, lasers and cold plasma distinguish from each other in generation processes by the order of the magnitude of the current amplitude,

some tenths of mA for cold plasma, and a few amps for lasers [6,10]. Non-equilibrium plasma processing at atmospheric pressure has been getting a great amount of attention because of its characteristics: small size, low temperature, low power consumption and easiness of generation at atmospheric pressure [11,12]. The atmospheric pressure glow discharge is called self-sustainable because of the secondary emissions of electrons from the cold cathode, mostly due to bombardment of positive ions [13, 14]. One of the technical problems in achieving stable and continual glow discharge at atmospheric pressure is that it tends to convert into arc discharge (thermal). This technical barrier can be overcome by covering one of the electrodes by dielectric materials; this is done to trap the charge and limit the total current density to prevent instability formation [13, 15]. Another technical barrier is the increase of pressure in the atmospheric pressure glow discharge due to the electrical breaking of gas at high pressure and maintaining a large volume discharge in glow mode, resulting in decreasing electron mean path [14, 16]. As mentioned at the beginning, product of pressure and distance between electrodes plays an important role in glow discharge. When *pd* is more than 20 Torr cm, electron mean path reduces so small in comparison to gas gap that seed electron can produce a large size avalanche before reaching the anode. This process produces enough positive ions to localize an electric field and convert discharge into micro-discharge [16, 4]. Electric discharge is the direct method to create non-thermal plasma. Since APGD is self-sustainable, non thermal and large-volume glow discharge, it is widely used in industrial applications. It is specifically used for thin film deposition, surface modification, deposition and sterilization [17, 18], etching of complex pattern for microelectronic and

micro-optical components, and for ozone generation [20, 23]. Plasma processes produce oxidizing radicals which help to treat gas pollutants [19].

In gas discharge physics, one of the phenomena is glow-to-arc transition. This occurs when applied current density is more than threshold value (approximately 50mA/cm^2), which leads to the volume reduction, and thermal heating of gas produces filamentary or arc discharge. In this regime, all the species, such as electron, ions, and neutrals, have the same temperature, which is higher than the room temperature. Thermal instability is another reason for glow-to-arc transition. The increase of electric field-to-density ratio increases the ionization rate and shifts electron energy to higher level. All these processes increase the temperature of gas and lead to runaway condition. Glow-to-arc transformation is a pressure sensitive phenomenon that occurs when current density crosses its threshold value at pressure above its threshold pressure [14, 4]. The stability of glow discharge also depends on the type of gas, for example, it is easier to develop stable glow discharge at atmospheric pressure in helium (monomer gas) than nitrogen, air and argon at same operating conditions. By changing the electrode configuration, one can produce stable homogeneous discharge in gases. In DC atmospheric glow discharge, in order to keep local current density under threshold value, a cathode electrode divides into a number of small parts and each part is stabilized by high resistance material [20]. Some researchers found that instability can also be controlled by the high flow rate of gas through discharge area [21]. However, the most effective technique is to control the instability by using dielectric material.

2.2.3 Dielectric barrier atmospheric- pressure glow discharge (DB-APGD)

Dielectric barrier discharge (DBD) is the easiest and widely used technique to produce glow discharge at atmospheric pressure. In this technique, at least one of the metallic electrodes is covered by dielectric material. DBD is also called "silent discharge" because of the absence of sparks which are followed by local overheating, generation of local shock waves and noise [22]. DBD can be distinguished into two configurations 1) volume discharge (VD), 2) surface discharge (SD). In volume discharge, micro-discharges are generated between two parallel plates and randomly distribute over the electrode surface, where the number of micro-discharges generated per period is directly proportional to applied amplitude of the voltage as shown in Fig.1.1. On the other hand, surface discharge generates on the dielectric plate and the counter electrode on the opposite side as shown in Fig. 1.2 [23, 80, 81].

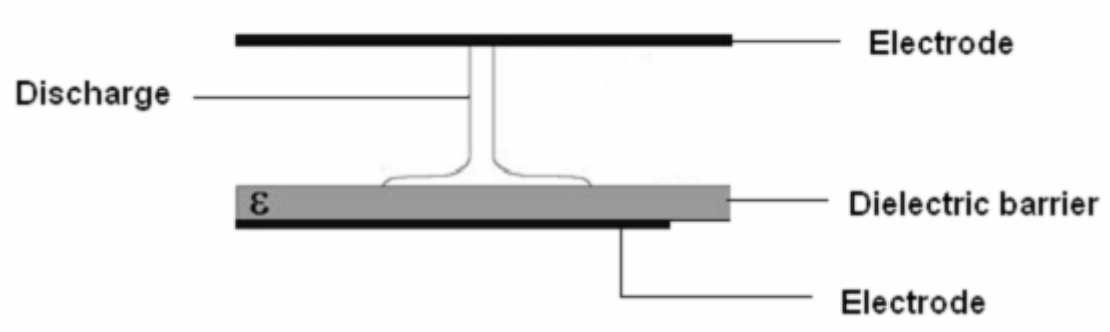

Figure 2. 1 Basic configuration of volume discharge [23]

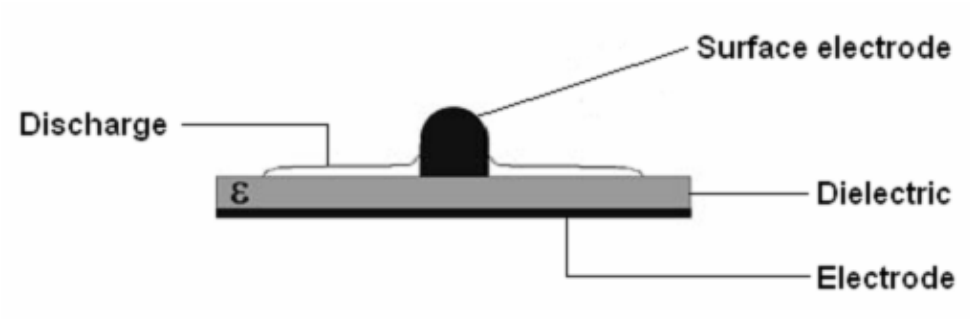

Figure 2. 2 Basic configuration of surface discharge [23]

The purpose of the dielectric material is to prevent high current occurrence in the channels of gas gap. The dielectric electrode can be made from glass, ceramic material, quartz and polymers [23, 22]. To generate discharge in the DBD, a.c. voltage can be applied from 1 kV to 100 kV and frequency from few Hz to MHz [23, 24]. The distance between electrodes can vary from a few mm to some cm, depending on the type of plasma (for example, it is 0.1mm in a plasma display, approximately 1mm for ozone generation, and several cm in CO_2 laser [23, 25]. Solid dielectric plate works as a series capacitor with the gas gap by putting limits to the voltage applied to the gas preventing transition to arc, and produces a large number of micro-discharges of a nanosecond duration [16,25]. The dielectric plate produces surface charge induced field which opposes the applied field by trapping the charge on the surface. This helps to extinguish the plasma before current density hits beyond its threshold value [16, 26]. In most of the cases, DBDs consist of micro-discharge filaments. They are very thin and directly proportional to the amplitude of applied voltage [23]. Once breakdown is done, charge starts building up on dielectric surface. This nanosecond duration of the breakdown decreases the electric field at the position of micro-discharge to a limit that the charge current at that point is interrupted. In DBD, little gas heating is done due to short duration

and the limited charge transport and energy dissipation. That is why a large part of electron energy can be utilized for exciting the gas molecules by leading to the chemical reaction [23].

Several researchers found that different modes of discharge in planar geometry depend on distance between electrodes, frequency and amplitude of applied voltage. Also, some of the modes of discharge are determined on the basis of the width of the discharge gap and thickness of dielectric barrier. The homogeneous discharge can be found in different modes and can be less affected by the amplitude and frequency of applied voltage [18, 27]. There are two modes based on the characteristic features.

1) Townsend discharge
2) Glow discharge.

When the gap width is not large and capacitance of dielectric is small enough, homogeneous barrier discharge takes place in Townsend mode. It is also distinguished by the position of maximum radiation intensity near the anode and small value of current [27]. Furthermore, the current profile will have one maximum or some maxima per half cycle [28, 27, 29]. The glow discharge can be formed when barrier capacitance is large and a gap is wide. It is also determined by one narrow current pulse of larger amplitude per half cycle. The spatial distribution of the radiation intensity in the phase of maximal current like bright negative glow, Faraday dark space, and the positive column, is similar to that for an ordinary DC glow discharge. The principle difference between these discharge modes is that in Townsend discharge the electric field gets less affected by spatial charge except in the phases of maximal current. On the other hand, in glow

discharge, electric field is strongly affected by spatial charge and the densities of charged particles are high.

In DBD at atmospheric pressure, the most common mode of discharge observed is streamer mode, occurring in an electronegative gas, e.g. air or oxygen [18, 30, 31]. In this mode, in each half-period of applied voltage, waveforms of discharge current show a reasonable series of sharp and rare spikes of approximately the same amplitude. When applied voltage is more than breakdown voltage, numerous streamers begin to excite simultaneously. This corresponds to every current spike, and excitation of the state suddenly goes down due to attachment and ion-ion recombination when applied voltage is less than breakdown voltage. This mode looks diffusive and transversely homogeneous because the steamers are randomly distributed in space [18]. One can also observe diffusive and transversely homogeneous discharge which resembles quasi-steady glow discharge with the large value of the parameter pd ($\geq$ 500-1000 torr mm) and low frequencies of applied voltage ($f <$ 100 kHz) in electropositive gases [18, 33-34]. When applied voltage crosses the breakdown voltage, the current waveform shows a single spike, which represents transversely uniform breakdown of gas in the electrode gap. Under these conditions, the voltage drop across homogeneous discharge column is greater than that across the cathode fall of a glow discharge [18]. In electropositive gases, we can also observe current filaments regularly distributed between two parallel electrodes, with the small value of product of pressure and distance ($pd \leq$ 500-1000 torr mm) and high frequency ($f \geq$ 100 kHz). The streamers in electronegative gases filaments are diffusive, and their transverse sizes are larger [18, 32].

2.2.4 Corona discharge

Corona discharge is another type of the discharge, which is generated between two electrodes. It includes two asymmetric electrodes, one highly curved like the needle or the wire and another is low curved. The purpose of the highly curved electrode is to make sure that high potential gradient is produced around one electrode for the plasma production. The name “corona” emerges from its appearance as lighting crown around the wire, when high negative voltage is applied to wire cathode at atmospheric pressure [23, 36]. The electricity corona discharge is an electric discharge accelerated by ionization of gas surrounding a conductor, which happens when conditions are not sufficient for complete electric breakdown or arcing in the presence of high strength of electric field [4, 37]. Coronas may be positive or negative depending upon the polarity of the voltage applied to highly curved electrode. The physics of negative and positive corona is remarkably different from each other. A positive corona generates in a uniform form across the length of electrode by emitting much of the emission in the form of ultraviolet, whereas the negative corona is non-uniform and dependent on the surface and unevenness of the electrode. Its mechanism is also similar to dc glow discharge where plasma is sustained by secondary electron emission because of positive ions movement towards the wire. This effect also is called as streamer, where high energy electron stays in front during propagation and leads to inelastic collision with the heavier particles, causing ionization of the gas. Corona discharge is self-sustaining and strongly non-equilibrium, both in terms of temperature and chemistry. The main reason is short time-scale of the pulses. The source plays an important role in the corona discharge. If the source is not pulsed, the discharge will produce heat, which will lead to non-equilibrium

stage transition into equilibrium and produce arching [23, 35, 4, 37]. Corona discharge has wide range of commercial and industrial applications such as sanitization of pool water, photocopying, flue gas cleaning, water purification, removal of dust particles from the gas or liquid by means of electrons attachment from the discharge to the dust particles, and destruction of volatile compounds that escape from paints [37, 23].

2.2.5 Micro hollow cathode discharge (MHCD)

To generate large volume discharge at atmospheric pressure, several research groups used different techniques such as radio frequency, microwave discharges, barrier discharge and corona discharge. In all the above techniques, the discharge is sustained by alternative or pulsed field, and in steady state discharges, the discharge is actuated by direct current power source [44]. Micro-hollow cathode discharge is one of the methods where discharge is activated by direct current. The micro-hollow discharge is classical version of hollow cathode discharge, in which pulse glow discharge is generated between two electrodes and separated by dielectric material with concentric hole in it [41]. The geometry is distinguished by hollow structure scaled to several hundreds of micrometer in the cathode. The discharge is influenced by cathode geometry, electrode material and operating condition. The cathode should be cylindrical or slit shape, whereas the shape of anode does not matter. Because of small and high pressure stability, it can be used as a small reactor to processes the gases. This discharge has high power density and generally operates at 1-5 W per hole [38, 39]. In the plasma research community, several researchers started to pay attention to the micro-hollow cathode discharge because of its advantages such as low power consumption, high power densities and high gas electron temperature. In addition to that, promising applications are miniature ultraviolet (UV)

and vacuum ultraviolet (VUV) sources, as well as material processing where small, confined plasma is required [40, 39]. It is also used in excimer radiation sources, sterilization of medicine, as an ionization source for ion mobility spectrometry or as excitation and ionization sources in emission and mass spectrometry [41, 42]. As per many researchers, because of hollow cathode effect, voltage found in micro-hollow cathode configuration is lower than in plane cathode configuration at the constant discharge current. At the same time, at constant voltage the discharge current is found to be orders of magnitude larger [43]. In the hollow cathode, effect starts generating in axial electric field between two electrodes, at very small current. In spite of that, when voltage rises the electric field transfers from axial to radial by accomplishing higher current at lower voltage. This effect drives electrons from the circular hollow cathode wall to the center of the hole by ionizing background neutral gas [42, 43]. In MHCD the discharge volume is highly intensified, stable and homogeneous in nature. Due to these conditions, neutral temperature reported is approximately 2000 K which is much higher than for dielectric barrier, corona and plasma jet. Still, it is lower than the arc discharge temperature. One of the motivations behind this research topic is the convenient use of this technology at atmospheric pressure where use of vacuum pump is avoided, which makes the system operation more simple and power efficient.

2.2.6 Capacitively coupled radio-frequency discharge (CCRFD)

In this type of glow discharge radio-frequency is applied to two plane parallel electrodes. In some arrangements discharge may be in touch with electrode, which is referring as “electrode” discharge. On the contrary, if electrode and discharge are separated by dielectric material, it is referred as “electrode less” discharge [14]. In

general practice, this plasma is operated at 13.56 MHz because international communication authorities assign this frequency to radiate a certain amount of energy without obstructing with communication [23, 4]. When the direct current is applied to the non-conducting material or the conductive electrode is covered with insulating material, discharge can still generate between the electrodes due to deposition of positive and negative charges. This technical problem is solved by applying alternating voltage to the electrodes, so that each electrode will perform as a cathode and anode alternately. In this way, the charge gathered during the first half-cycle can be partially neutralized by opposite charge in the next-half cycle. To maintain quasi-continuous discharge, the frequency should be maintained high enough so that the period of alternative voltage is less than the time required to insulator charge up. The numerically calculated frequency value is greater than 100 kHz to maintain continuous discharges. It has many industrial applications such as etching and deposition as one of many steps in the production chain of many circuits [45, 35, 23].

2.3 Stable glow discharge at atmospheric pressure

In the beginning of plasma research it was thought that glow plasma was stable only at lower pressure. Okazaki found that by using two parallel metal electrode structure covered with the dielectric material, stable glow discharge can be produced at atmospheric pressure, using helium as dilute gas, and applying more than 1 kHz frequency [?]. Different methods are used to produce stable glow discharge at atmospheric pressure under different conditions such as electrode shape and material, applied frequency and type of dilute gas. In brush style, top electrode is made from tungsten and stainless steel wires. The stable glow is discharge produced at 3000Hz

applied frequency in methane and hydrogen in the presence of helium as diluting gas. It is observed that with this technique carbon films with the good properties were deposited on the quartz electrode at atmospheric pressure. With this development in production of glow discharge at atmospheric pressure, many researchers were attracted towards this technique (parallel plate electrode covered with dielectric material) and they used it for material technologies such as surface activation [74, 75], deposition [15, 76, 77, 78] and synthesis [77]. It is also used for environmental applications such as gas cleaning, water purification and biomedical applications for instance bio-sterilization [79]. The schematic of electrode dielectric configuration is shown in fig 2.3.

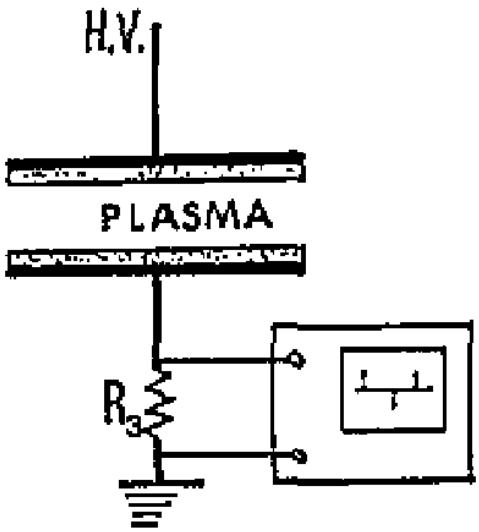

Figure 2. 3 Schematic of plasma electrode dielectric arrangement with electric circuit [40]

In further research of plasma, it is observed that in some gases like air, nitrogen, methane and oxygen, atmospheric glow discharge becomes unstable and transits to filamentary discharge. This is caused by secondary electron discharge [30, 46, 9]. The transition of plasma from one phase to another is explained by Kekez in 1970 [?]. According to Kekez's observation (Fig 2.4), the discharge begins with the Townsend

discharge at atmospheric pressure. It then transits from glow discharge (first glow) to filamentary (second glow) and then finally to arc discharge. It is also reported that Townsend-to-arc discharge transition is dependent on the gas type, gas pressure, applied voltage and the discharge gap length [46].

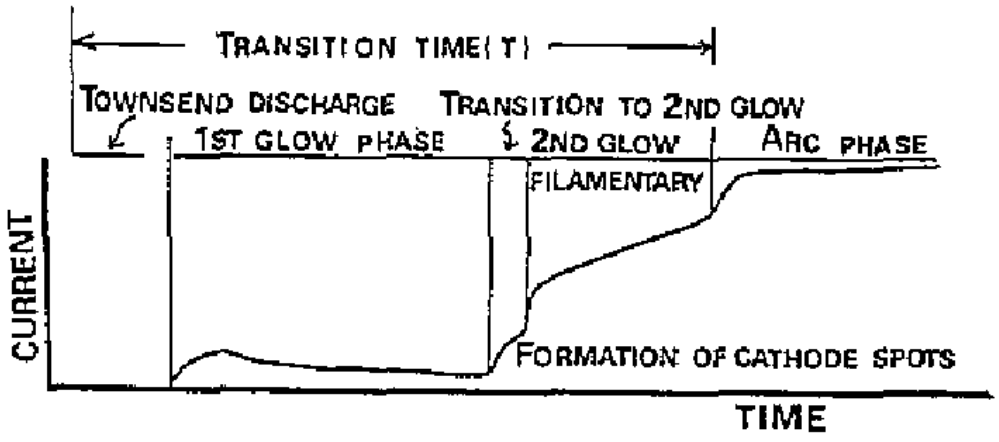

Figure 2. 4 Transition from a glow discharge to arc discharge [46]

2.4 Conversion of methane into higher hydrocarbons

It is possible to generate stable glow discharge at atmospheric pressure and room temperature in DBD. Because of its good characteristics such as high non-equilibrium of plasma, it is considered a promising technology to generate hydrogen and higher hydrocarbons from methane. Methane is considered an important energy source because of higher H/C ratio 4 in comparison with coal and oil [54]. It has always been a challenge for direct conversion of methane because of the high stability of the C-H bond in methane molecule. To overcome this problem, several plasma technologies have been studied by using different catalysts and co-feed gases in the methane to improve the methane conversion to higher hydrocarbons. Oxygen [68,70] ,carbon dioxide [67,69,73], hydrogen [68], and nitrous oxide have been used as co-feed in microwave, radio frequency

discharge, corona discharge and DBD [72,73]. The DBD can produce a series of hydrocarbons in the presence of a larger volume discharge as compared to the corona and microwave discharge [47]. It is found that methane conversion can be increased using oxygen, which activates methane during DBD.

On the other hand, excess oxygen can oxidize the intermediate product and produce carbon dioxide and water. The strong oxidation effect in the reaction can be controlled by adding catalysts and implementing proper conditions to get the desired products [47, 48, 49]. The direct methane conversion is also possible in DBD because of its high electron energy (up to 10 eV) to break the C-H bond. The conversion of methane into higher hydrocarbon was also studied under the influence of different flow rates (20 mL/min and 40 mL/min) and applied voltage (up to 11kV). It is seen from the experiment that at a constant frequency and applied voltage, if we increase the flow rate than there is always decrease in methane conversion because of a lower reactor residence time [48]. Increase in applied voltage produces less effect on the product selectivity and increases the conversion in both cases. In DBD, the main products of methane decay are higher hydrocarbons such as C_2H_2, C_2H_4, C_2H_6, C_3H_6, C_3H_8, C_4H_{10}, and C_3H_6 [50]. Becker and coworkers explained the sequence of reactions that occur during the methane conversion in gas phase to produce higher hydrocarbons:

$$CH_4 \rightarrow C_1 \rightarrow C_2 \rightarrow C_4 \rightarrow C_6 \rightarrow C_n$$

where C_1=CH_3, and C_6 and C_n are mononuclear and poly-nuclear aromatic hydrocarbon species respectively.

The conversion of methane was also studied in the presence of ethane in DBD [48]. It was observed from the experiment that the presence of 10% or 20% ethane

improves the methane conversion as compared to pure methane. This is due to the presence of a weak single bond between two carbon atoms in ethane molecule as compared to the C-H bond in methane. This indicates that methane is more quickly activated by ethane derived active species as compared to species formed from methane. The hydrogen production also increases because of coupling reactions forming C_2-C_4 paraffins. Furthermore, it also increases propane selectivity by increasing availability of active C_1 and C_2 species for coupling [48]. The study shows that direct methane conversion into fuel using DBD also produces polymerized carbon film and carbon black in the reaction, even in the presence of co-fed CO_2 as an oxidant [47, 51]. This problem can be overcome by applying zeolite A in the DBD [47, 52, 53]. The variation in the CH_4/CO_2 feed ratio shows an effect on the conversion of CH_4 and CO_2 in the presence of zeolite A. The decrease in the feed ratio surges the conversion rate and, on the other hand, an increase in the feed ratio increases the yield of H_2 and C_2-C_4 hydrocarbons. The experimental results indicate that the feed ratio has an effect on the molar ratio of H_2/CO. When the feed ratio varies from 1/1 to 3/1, the molar ratio boosts immediately from 0.7 to 3.1 [47]. It is also proved that applied power plays an important role in methane conversion and production of hydrocarbon in the presence of CO_2 in DBD. In co-axial DBD, the increase in power increases CH_4 and CO_2 conversion with the decreasing production of C_2-C_4 hydrocarbons. This indicates that at higher power, lower hydrocarbons convert into higher hydrocarbons. The experimental results show that acetylene is not a major product of plasma reaction. It has been proved by many researchers that the use of zeolite as a catalyst can improve ethylene/ethane and propylene/propane ratio in hydrocarbon reaction [47, 55, 52]. There is no effect of power

increase on these ratios. On the contrary, H_2/CO was increased in syngas production [55]. The effect of hydrogen on the methane conversion in pulse discharge was also studied by Kado el al. [54] under the reaction conditions of 10 cm^3/min total flow rate, 1.5 mm gap and applied current 4.0 mA. It was found that output products of methane conversion do not change much in hydrogen presence as compared to the pure methane conversion. During the experiment, hydrogen concentration varied from 0 to 90% at total flow rate of 10 cm^3/min. The results indicate that there is only increase in methane conversion and C_2 yield above 50% concentration (CH_4:H_2=1:2). At 80% hydrogen concentration, two forms of discharge were observed: (a) stable pulse discharge and (b) stationary discharge (corona discharge). The methane conversion reduces slightly under the influence of pulsed discharge. Under the influence of stationary discharge, methane conversion shows significant reduction with acetylene selectivity. However, selectivities of ethane and ethylene increase. These observations pointed out that overabundance of hydrogen in methane obstruct the electron collision with the methane molecule by decaying hydrogen into an excited atom [54].

Since the 1980s, much research has been done towards methane conversion into more valuable hydrocarbons by Franser et al., Bhatngar et al, and Larkin et al. [55]. To achieve the desired results from methane conversion, different methods have been used. The O/P product is dependent on the reaction occurring inside the plasma. Therefore, it was important to propose reaction pathways, which will give more insight into the application of methane coupling [56]. Kim and co-worker proposed the kinetic mode of methane decomposition (Fig. 2.5) in coaxial DBD setup in which the quarts tube acts as

dielectric material. The experiment was carried out at applied voltage of 17kV, feed flow rate of 6 mL/min, and residence time of 100 sec [50].

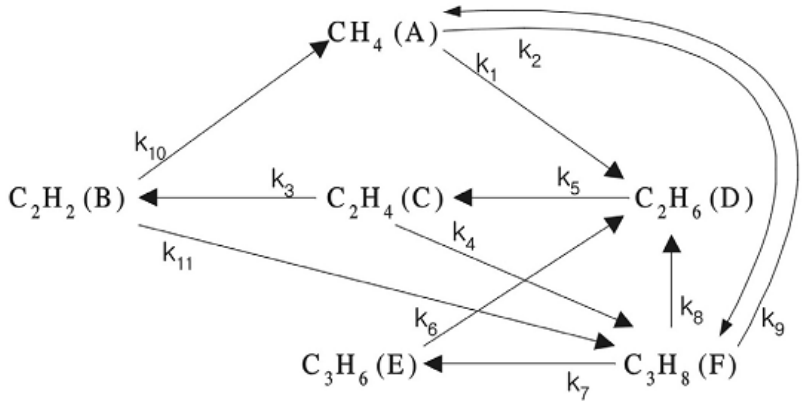

Figure 2. 5 The suggested reaction path way for methane decay in DBD [50]

Here k_1-k_{11} are rate constant calculated by comparison between the calculated and experimental values, using the least square method.

2.5 Conversion of propane into lower hydrocarbon and syngas

The conversion of propane into lower hydrocarbons and syngas also attracted many research groups. Different types of plasma techniques have been used to activate the propane such as sliding discharge reactor at atmospheric pressure and low temperature [60], cold plasma in micro-reactor [57], and catalytic reaction, e.g. vanadia catalyst over mesoporous silica [5]. In accordance with studies conducted in this area, it has always been a difficult challenge to convert alkenes because of the strong bond between C-C and C-H atoms [66]. The problem can be solved by using catalytic processes in which oxygen and high temperature are generally used. In spite of that, this process has some difficulties: (a) in the presence of oxygen, the sintering process causes a loss of catalytic activity, (b) coke formation, and (c) they assist non selective combustion

in the presence of oxygen [57]. DBD in two parallel electrodes setup demonstrates the possibility to overcome these limitations because of its characteristics, for example, gas temperature close to room temperature and high electron energy to activate hydrocarbon. On this principle, Agiral and co-worker used the plasma micro-reactor made from Pyrex glass shown in Fig 2.6. The use of the micro-reactor allowed researchers to work at higher pressure than those in the conventional low pressure technique. It also uses less oxygen at low temperature, allows the generation of dense and uniform plasma and better control of residence time [58, 59, 57].

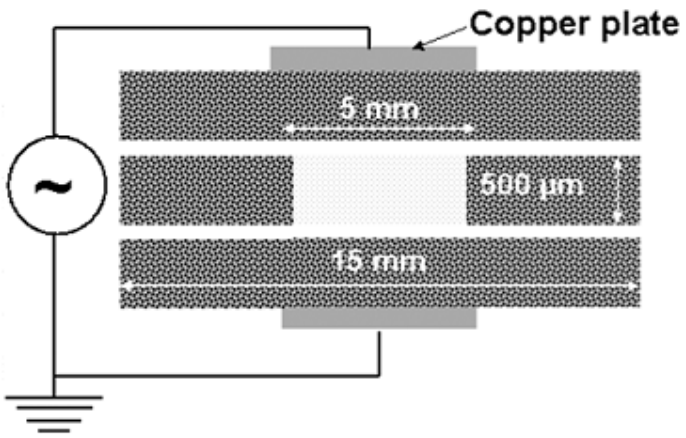

Figure 2. 6 Schematic of cross section view of micro discharge reaction [57]

The experimental results show increase in propane conversion with the increase in power I/P under the conditions of 1 atm, 25^0C, flow rate 10 mL/min and 10% propane in helium [57]. When 1% oxygen is added in the mixture, the propane conversion increases by 7% mole at the same condition. This indicates that propane conversion increases in the presence of oxygen [57].

Presently hydrogen is considered the best option for fuel cell and automotive applications in the future [61, 62]. There are many methods for pure hydrogen production, e.g. partial oxidation with oxygen (PO), steam reforming (SR), steam reforming with oxygen (SRO), CO_2 reforming (CDR) and CO_2 reforming with oxygen (CDRO) [60]. Among these technologies, SRO draws more attention because of the following characteristics: low energy requirements, the high space velocity, a lower process temperature than at partial oxidation. Control over the H_2/CO ratio can be obtained by regulating the inlet gas ratio [63, 64]. Ouni et al. used non-thermal plasma reforming process to decay the propane by using the sliding discharge reactor [?]. It operated at low temperature with atmospheric pressure and flow rate of 80 L/min. The byproduct of the reaction was 50% hydrogen, and less than 6% hydrocarbon was measured. The inlet gas temperature was maintained at 150^0C. The endothermic reaction that occurred during the propane steam reforming is described by following equation:

$$C_3H_8 + 3H_2O \rightarrow 7H_2 + 3CO$$

The experimental results prove that the final product is dependent on the steam-to-propane ratio. With increasing H_2O/C_3H_8 ratio, the conversion decreases. The higher C_2-hydrocarbon and methane were found when the ratio was maintained at 4. The formation of CO_2 also occurred because of water gas shift reaction at the same condition. These results indicate that in propane conversion, the first step is formation of lower hydrocarbon and then the reaction occurs between lower hydrocarbons. On the basis of identification and quantification of the O/P product, following reactions have been proposed:

$$C_3H_8 \rightarrow 3H_2 + C_2H_2 + C$$

$$C_3H_8 \rightarrow 2H_2 + C_2H_4 + C$$

$$C_3H_8 \rightarrow 2H_2 + CH_4 + 2C$$

$$CO + H_2O \rightarrow H_2 + CO_2$$

Rosach et al. [65] used a coaxial cylindrical reactor for the silent electric discharge to increase the flame speed and stabilize flame in the combustion of gaseous hydrocarbon fuel under the effect of plasma. Two mechanisms were identified for fuel cracking and activation: (1) electron collision with parent molecule produces excited radical and molecule fragments, and (2) the collision between electrons and neutral species produces ions which promote ion-molecule reactions. The former mechanism is explained using possible reactions in ethane and propane as follows:

$$e + C_2H_6 \rightarrow 2CH_3\bullet + e$$

$$e + C_2H_6 \rightarrow H_3\bullet + CH_2: + H\bullet + e$$

$$e + C_2H_6 \rightarrow CH\bullet + CH_3\bullet + H_2 + e$$

$$e + C_2H_6 \rightarrow C_2H_4^* + H_2 + e$$

$$e + C_3H_8 \rightarrow C_2H_5\bullet + CH_3\bullet + e$$

$$e + C_3H_8 \rightarrow 2CH_3\bullet + CH_2: + e$$

$$e + C_3H_8 \rightarrow C_3H_7\bullet + H\bullet + e$$

The output (radicals) of these reactions can further decay ethane and propane or their decomposition product to get more active species. This is explained by following reactions:

$$H\bullet + C_2H_6 \rightarrow C_2H_5\bullet + H_2 \text{ or } CH_3\bullet + CH_4$$

$$H\bullet + C_3H_8 \rightarrow n\text{-}C_3H_7 + H_2 \text{ or iso-}C_3H_7 + H_2$$

$$H\bullet + C_2H_2 \rightarrow C_2H_3 \text{ or } C_2H + H_2$$

$$H\bullet + C_2H_4 \rightarrow C_2H_5\bullet \text{ or } C_2H_3 + H_2$$

$$H\bullet + C_2H_5\bullet \rightarrow C_2H_4 + H_2 \text{ or } 2CH_3\bullet$$

$$CH\bullet + CH4 \rightarrow C_2H_4 + H\bullet$$

$$CH\bullet + C_2H_4 \rightarrow C_3H_2 + H_2 + H\bullet \text{ or } C_2H_2 + CH3\bullet$$

$$CH\bullet + C_2H_6 \rightarrow \text{Products (e.g., } C_2H_2 + CH_4 + H\bullet)$$

$$CH\bullet + C_3H_8 \rightarrow \text{Products (e.g., } C_3H_6 + CH_2: + H\bullet)$$

$$CH_2: + C_2H_6 \rightarrow C_3H_8 \text{ or } CH_3\bullet + C_2H_5\bullet$$

$$CH_2: + C_3H_8 \rightarrow CH_3\bullet + \text{n-}C_3H_7\bullet \text{ or n/iso-}C_4H_{10}$$

$$CH_3\bullet + C_2H_6 \rightarrow CH_4 + C_2H_5\bullet$$

$$CH_3\bullet + C_3H_8 \rightarrow CH_4 + \text{n-}C_3H_7\bullet \text{ or } CH_4 + \text{iso-}C_3H_7\bullet$$

The detection and identification of radical species produced from the decay of pure hydrocarbons is a challenging job, and such studies have rarely been reported in the literature [65].

2.6 Summary of the previous work and objectives of this study

The literature review shows that dielectric barrier discharge (DBD) is the most promising type of plasma for combustion applications. It has been shown that addition of small amounts of oxygen to methane and propane significantly improves the yield of desired products. The use of this method for industrial applications is hindered, however, by the high cost of oxygen. The overall goal of our research is to explore the feasibility of using air instead of oxygen in this process. For this purpose, we investigate the influence of the DBD frequency on the reforming of methane, propane, and their mixtures with small amounts of air.

The specific objectives of our study are:

- To develop an experimental setup with a cooled reaction chamber which allows experimentation under controlled conditions.
- To investigate the effect of DBD frequency on the plasma-assisted reforming of pure methane and propane at atmospheric pressure.
- To investigate the influence of small (5% and 10%) air amounts on the plasma-assisted reforming of methane and propane at different frequencies of DBD.
- To demonstrate that plasma treatment of fuels enhances the combustion rate and structure of methane-air and propane-air diffusion flames at different A/F ratios.

Chapter 3 EXPERIMENTAL SETUP

3.1 Overview of the experimental setup

This chapter describes the experimental setup for one common configuration that is used for generating high-pressure plasma, specifically, dielectric-barrier atmospheric-pressure glow discharge (DB-APGD). The setup is configured to study the effect of DBD on the gases (methane and propane) and their mixtures with air at atmospheric pressure. The schematic and photograph of the setup are shown in Fig. 3.1. and Fig 3.2, respectively.

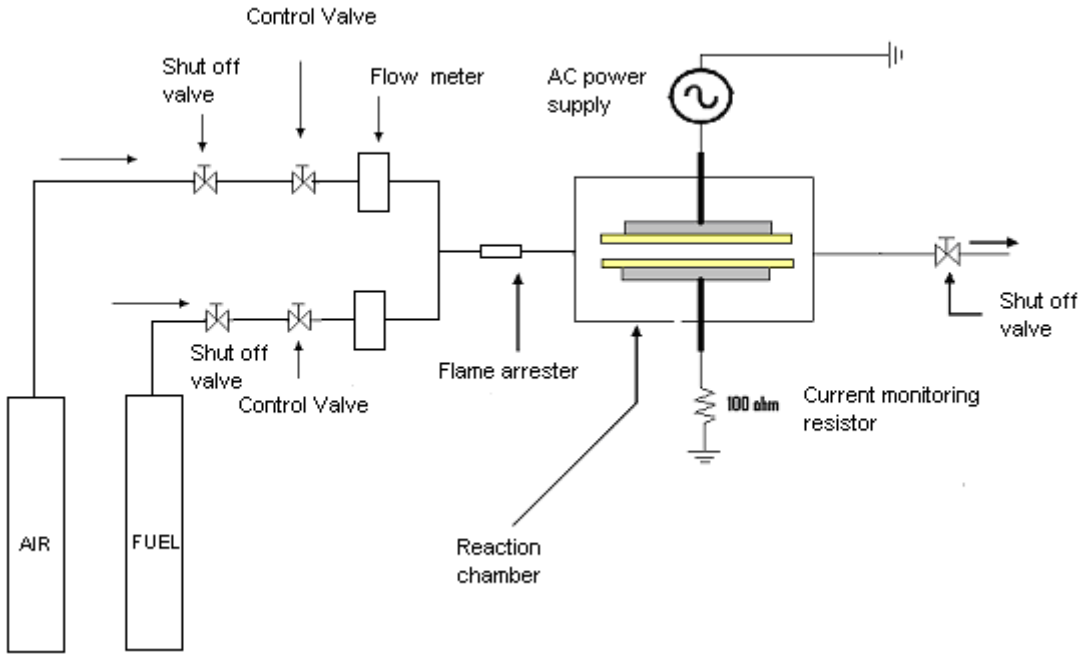

Figure 3. 1 Schematic diagram of the experimental setup

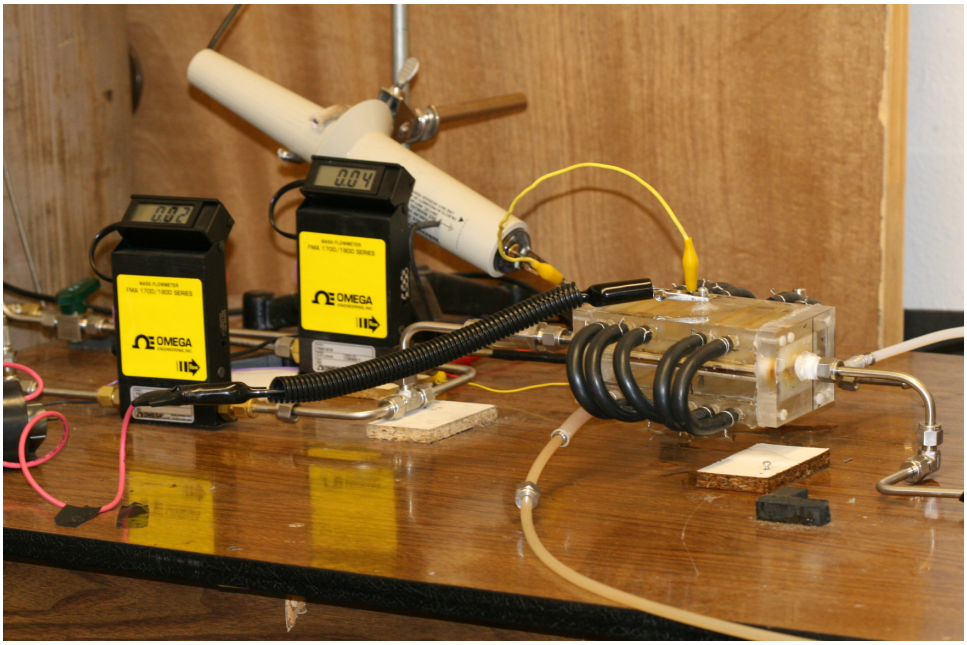

Figure 3. 2 Photograph of the experimental setup

The experimental setup is based on the previous works of Raja el al. [78]. It is the modification of the basic parallel plate configuration to produce glow discharge at atmospheric pressure. As per the DBD concept we used two aluminum parallel plates as electrodes with thickness 0.172 cm and dimensions 8.3 cm x 3.3 cm. The inner faces of the electrodes are covered by 0.15 cm of thick high-purity dielectric alumina (Al_2O_3, 99.5%) to trap the charges on their surfaces and to maintain the stability, i.e. avoid the glow-to-arc transition phenomenon [16]. The dielectric plate has a relative dielectric constant (ϵ_r) of 9.5, thickness 0.15 mm and dimensions 11.5 cm x 5.5 cm. The purpose of having a larger area for dielectric plate than aluminum electrode is to avoid the arching at the edges of plate. The two assemblies (electrode-dielectric) are separated from each other by a distance of 3 mm throughout the experiments. The reason to select these materials for electrode and dielectric plate is because of their high thermal and electrical

conductivity at the room temperature. The calculated value for dielectric barrier capacitance is 177.3319×10^{-12} (for calculation refer appendix A). During the experiment, the reaction chamber is powered by AC power source through a top electrode. The lower electrode is grounded through 100 Ω resistor, which is connected in series to measure the discharge current in the circuit. The input signals voltage and voltage fall are measured by Tektonix TDS 1012 Digital Oscilloscope and data are recorded by a computer.

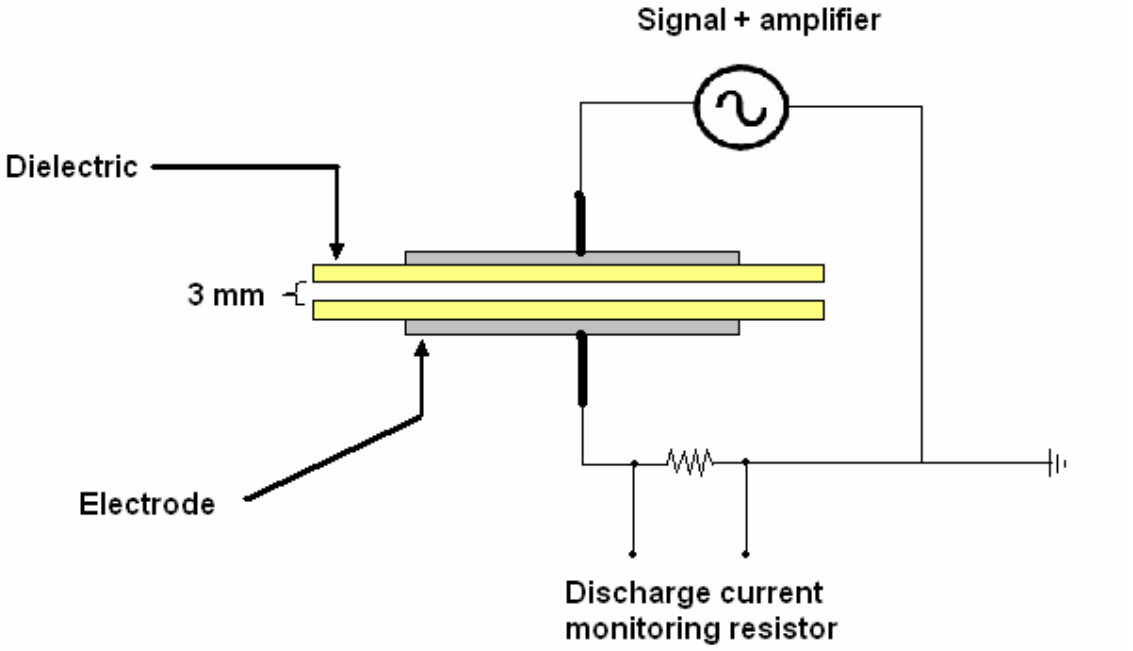

Figure 3. 3 Schematic of dielectric barrier discharge system [35]

3.2 Reaction chamber

The reaction chamber used for the experiment is shown in Fig.3.4. It is made from acrylic material. It is a rectangular box of dimentions13.97cm X 7.26cm X 6.0cm, made by connecting four pieces of acrylic sheets leaving the center space empty to place the electrode assembly. It is an open system, closed from all the sides, which has one inlet and one outlet on its opposite sides. The reaction chamber walls are connected to each

other using weld on solution and Swagelok's plastic screw. The main purpose of utilizing plastic screws is to avoid arching inside the reaction chamber during high voltage reaction. The electrodes are kept apart by making two grooves at 3mm distance on each face of the smaller side of the reaction chamber. The vertical and horizontal movement is restricted by making a threaded hole at the center of the top surface and infusing a bolt. The bolt also acts as a part of the electrode because it is connected to the electrode assembly and high voltage current can be applied to the head of the bolt. On the opposite side of the electrode, we used the same arrangement for the grounding purposes. The leak in the chamber is taken care of by applying transparent silicon room temperature vulcanization (RTV) on all the joints of reaction chamber. The temperature in the reaction chamber is controlled by modifying the chamber design and introducing a water cooling system in the walls of reaction chamber. The water flow rate was maintained at 0.9 L/min. The cooling system is introduced into the reaction chamber by drilling five horizontal through holes in the top and six holes in the bottom wall of the reaction chamber, parallel to the electrodes. By creating parallel hole we can cover maximum surface area and transfer maximum amount of heat by conduction. All the holes are connected using high temperature rubber tubing with I.D 0.635cm and O.D 0.96 cm. The connections are made in such a way that the water will flow in the spiral form around the reaction chamber.

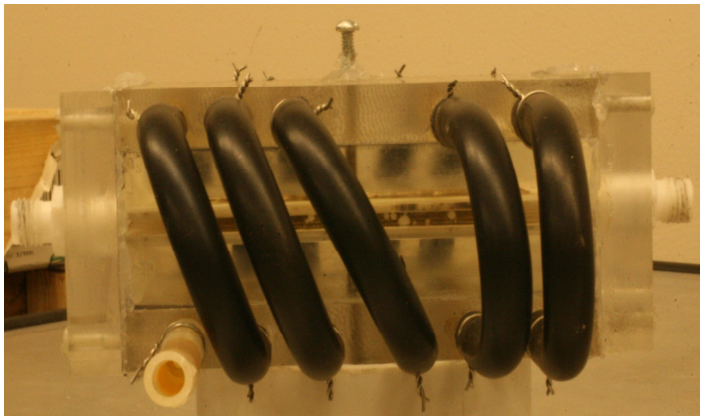

Figure 3. 4 Side view of the reaction chamber

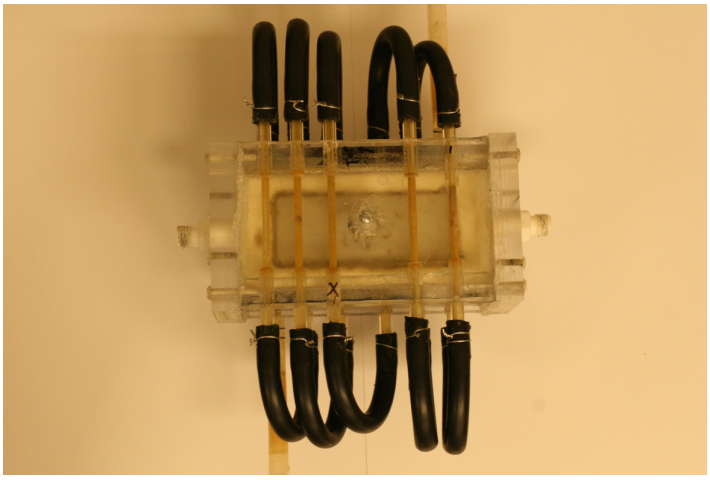

Figure 3. 5 Top view of reaction chamber

The important part of the reaction chamber is the electrode assembly (Fig. 3.6). This includes an aluminum electrode (thickness 0.15cm, area 8.5 cm x 3.5 cm) and a ceramic (alumina) plate (thickness of 0.172 cm, area 11.5 cm x 5.5 cm) as a dielectric barrier. There should be proper face-to-face contact between them to generate a good amount of plasma. After many tests, we decided to use H20E EPO-TEK silver conductive epoxy because of its thermal and electrical properties. It is a mixture of two parts: part "A" (epoxy resin and silver powder) and part "B" (hardener and silver powder). We used 1:1 parts by weight, after applying silver epoxy between aluminum plate and ceramic plate. We kept that in the oven for 15 min at 120^{o} C to cure. Before

assembling two plates together, we drilled a threaded hole in the center of aluminum plate for proper contact with screw so that it can hold assembly in fixed position during the reaction.

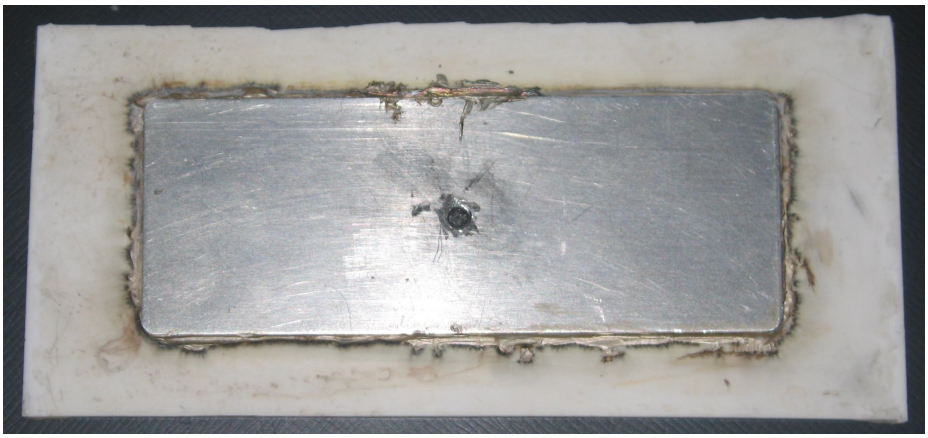

Figure 3. 6 Actual electrode assembly

3.3 Measuring equipment

3.3.1 P6015A 1000X high-voltage probe

The purpose of this device in the experiment is to measure the voltage generated across the discharge. It is directly connecting to the top electrode to cross check the discharge voltage recorded by digital oscilloscope. The P6015A is a 100 MΩ, 3.0 pF high voltage probe with 1000X attenuation. Because of its high input resistance of 1 MΩ and high input capacitance of 7pF to 49 pF, it adds high voltage measurement capability to the oscilloscope and other measuring devices [35].

.

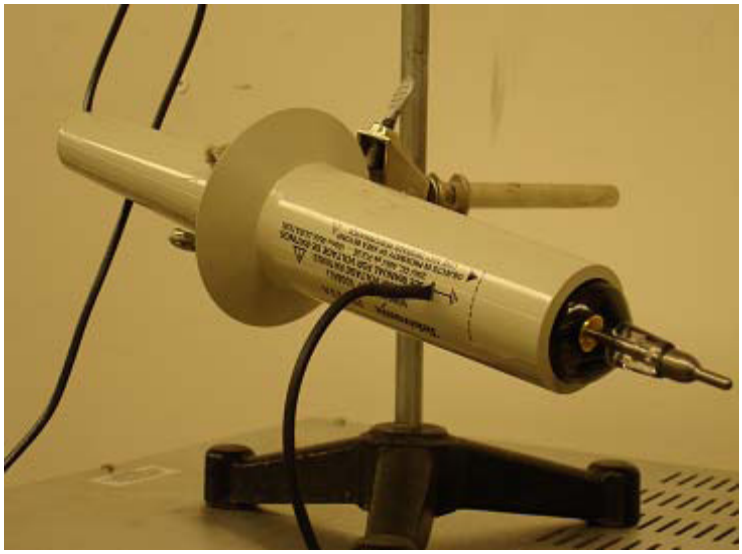

Figure 3. 7 High voltage probe (P6015 A 1000X)

3.3.2 Function Generator (AGILENT 33120A)

Agilent 33120A Function/Arbitrary waveform generator uses the latest direct digital-synthesis technique to create a stable and accurate output signal for clean, low-distortion sine waves. It also provides fast rise and fall time, square wave and linear ramp waveforms down to 100 μHz. It also provides AM, FM, and FSK modulation capabilities, as well as sweep and burst output modes. The 33120A provides easy access to standard sine, square, ramp, and triangle waveforms; in addition to that, it can generate custom waveforms using the 40 MSa/s, 12 bit, 16,000-point arbitrary waveform function. Additionally, the instrument provides the added convenience of a built-in frequency counter. This allows more accurate determination of output frequency than is possible with a simple calibrated dial. The important part of the function generator is (VCG) voltage-controlled generator that generates accurate sine, square, or triangle waves over the 100 Hz to 15 MHz range. With this feature of variable symmetry of the o/p

waveform, it modifies the instrument to a pulse generator capable of producing rectangular waves or pulses, ramp or saw-tooth waves, and slewed sine waves [35].

Figure 3. 8 Agilent 33120 A

3.3.2 Tektronix TDS 1012 Digital Oscilloscope

The principal use of an oscilloscope is to display a graph of i/p voltage on the vertical axis as a function of time on the horizontal line. The used device has a band width of 100 MHz and 1GS/s sample rate. In addition to that it comes with advance triggering and auto set menu with wave form selection.

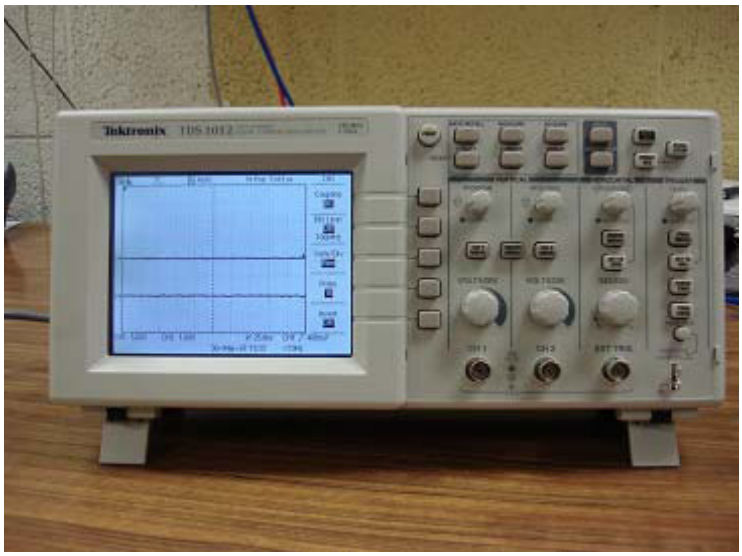

Figure 3. 9 Digital oscilloscope (Tektronix TDS 1012)

3.3.4 Agilent 3000 Micro Gas Chromatograph

The Agilent 3000 (Fig. 3.10) is a powerful GC solution that provides fast, accurate, and reliable analysis of gas sample on-line right at the sampling point. It is suitable for the fast analysis of gas streams in different processes, e.g. fuel cell development, coal mine safety monitoring, and the hydrocarbon processing industry, including refineries, natural gas production and distribution, chemical operations, and oil and gas exploration. The micro GC can be found in 1-to-4 channel that performs analyses in seconds. It also comes with the powerful Aglilent Cerity Networked Data system software for chemical QA/QC, which helps in data analysis and controls the instrument. The heart of the instrument is a GC module, consisting of heated injector, sample and reference columns, flow control valving, thermal conductivity detector (TDC) electronic pressure control (EPC). It comes with an external 10-micron filter to protect from condensable vapors because of its micro machined construction of the GC module. There are three important processes taking place during analysis: injection, separation, and detection. The 3000 micro GC gas chromatograph we used contains four columns described in Table 3.1.

Table 3. 1 Specification of gas chromatograph columns

	Injector Type	Carrier gas	Column Type	Detector Type	Inlet Type
Channel A	Back flush	Argon	Molecular Sieve	TCD	Heated
Channel B	Back flush	Helium	Molecular Sieve	TCD	Heated
Channel C	Back flush	Helium	Plot U	TCD	Heated
Channel D	Back flush	Helium	Alumina	TCD	Heated

Figure 3. 10 Agilent gas chromatograph 3000

Chapter 4 EXPERIMENTAL RESULTS

4.1 Dielectric barrier discharge in methane

The experiment was performed using pure methane gas. The flow rate was controlled by using a shut-off valve, a needle valve and a flowmeter (Omega Engineering), which were connected in series before the reaction chamber. The flow rate maintained throughout the experiment was 0.2152 L/min, selected on the basis of stoichiometric air/fuel ratio for complete combustion (Table 4.1).

Table 4. 1 Calculation of air fuel ratio for methane and propane

Fuel	MW fuel	Mw air	(A/F)s	Rho (kg/m3)	K factor for fuel	Q_fuel (lpm)	Q_air (lpm)	(A/F)o	Φ
CH4	16	28.967	17.23537	0.715	0.7175	0.21525	1.9	15.96257	1.079736
C3H8	44	28.967	15.66851	1.967	0.35	0.07	1.68	15.77631	0.993167
air				1.293					
CH4 lean					0.7175	0.21525	2.15	18.07	0.953811
CH4 rich					0.7175	0.21525	1.7	14.26	1.208651
C3H8 lean					0.35	0.091	2.25	16.249	0.964276
C3H8 rich					0.35	0.091	1.95	14.082	1.112663

Initially, to ionize the gas, a breakdown voltage of 20 kV was applied at peak to peak at a frequency of 6 kHz. Once the gases are completely ionized and plasma is uniformly distributed over the electrode surface, we reduced the voltage by keeping the same frequency to a point where the discharge can stay in homogeneous state. First set of reading was taken at 9 kV and 6 kHz frequency and analysis of specimen was done by gas chromatography. The other sets of reading were taken by increasing applied frequency up to 10 kHz with an interval of 1 kHz and maintaining the voltage constant.

For each set of data, 2 to 3 sets of data were collected for the samples under the same conditions. We used the average reading to minimize the errors. The O/P results of different reactions are plotted in the Fig. 4.1 with respect to frequency. The applied voltage and current waveforms with respect to time are shown in Fig. 4.2.

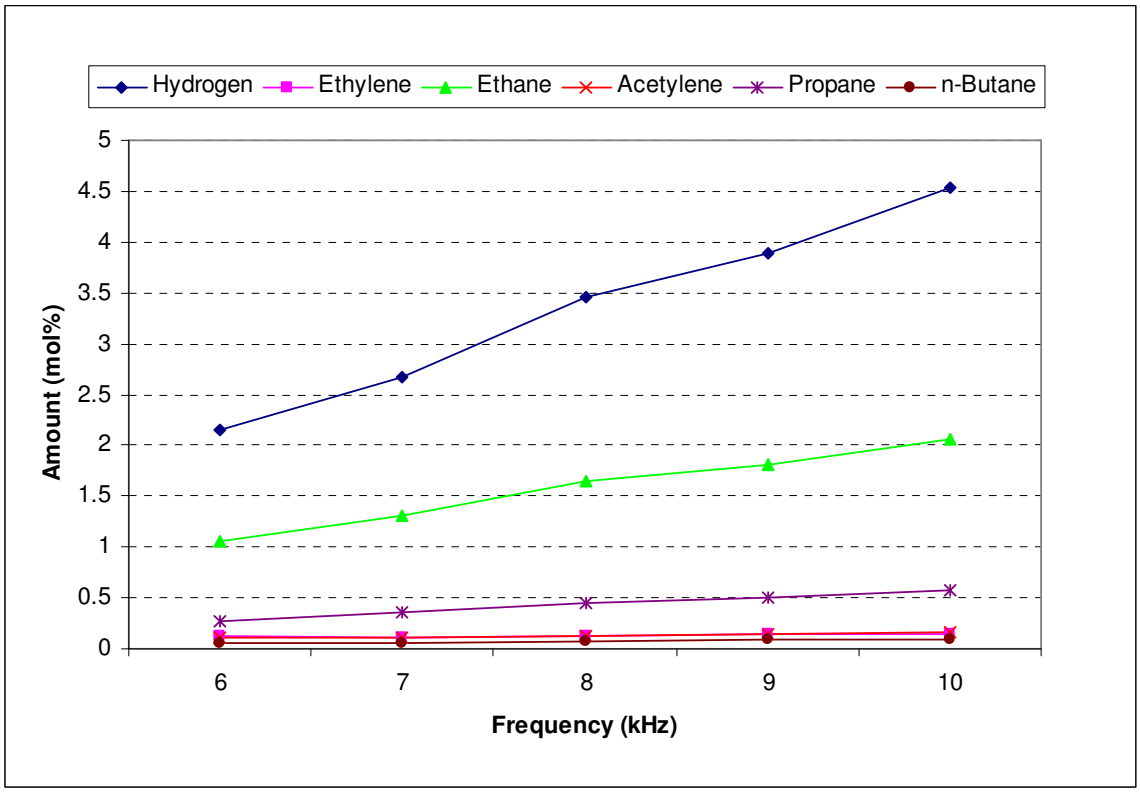

Figure4. 1 Plot for species amount (mol%) at different frequencies for methane

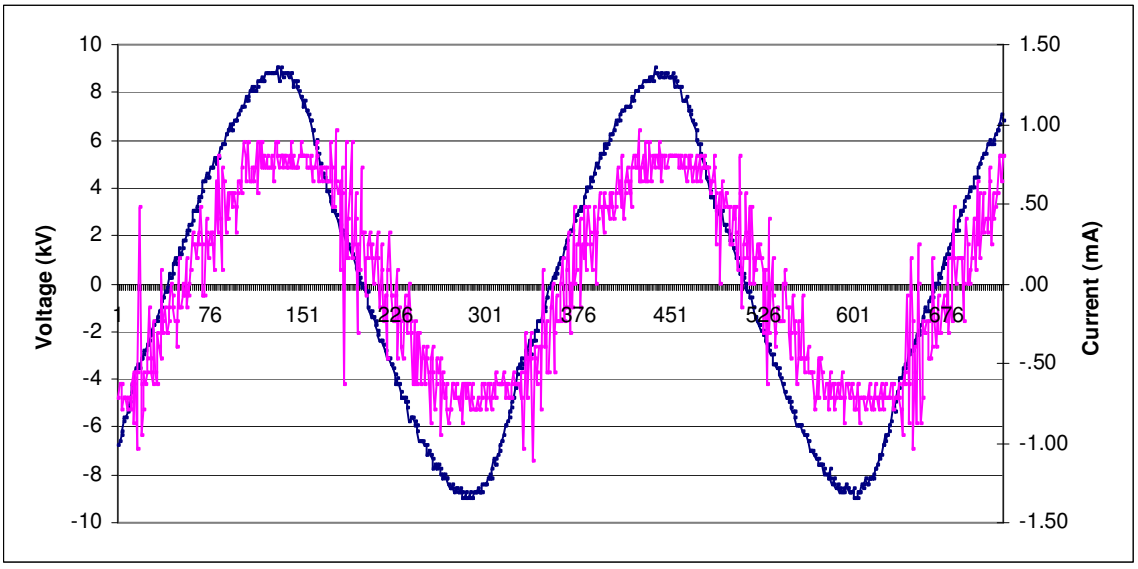

Figure 4. 2 Plot for voltage and current waveform at 9 kV, 8 kHz in methane

4.2 Dielectric barrier discharge in methane and air (5%) mixture

In this experiment, we added an extra air flow parallel to methane flow, connecting them together using Swagelok tee joint, which is shown in Fig.3.1. Additional flow line also includes a shutoff valve, a needle valve and a flow meter in a series to control the flow rate of air. The methane flow rate was maintained at 0.215 L/min and air flow rate at 0.095 L/min (which is 5% of 1.90 L/min). We followed the same procedure by flushing the chamber with the mixture to ensure purity of the sample. The breakdown voltage was found to be 21 kV peak to peak at 6 kHz frequency. The sets of samples were collected by maintaining a constant voltage at 9kV and changing frequency from 6 kHz to 10 kHz.

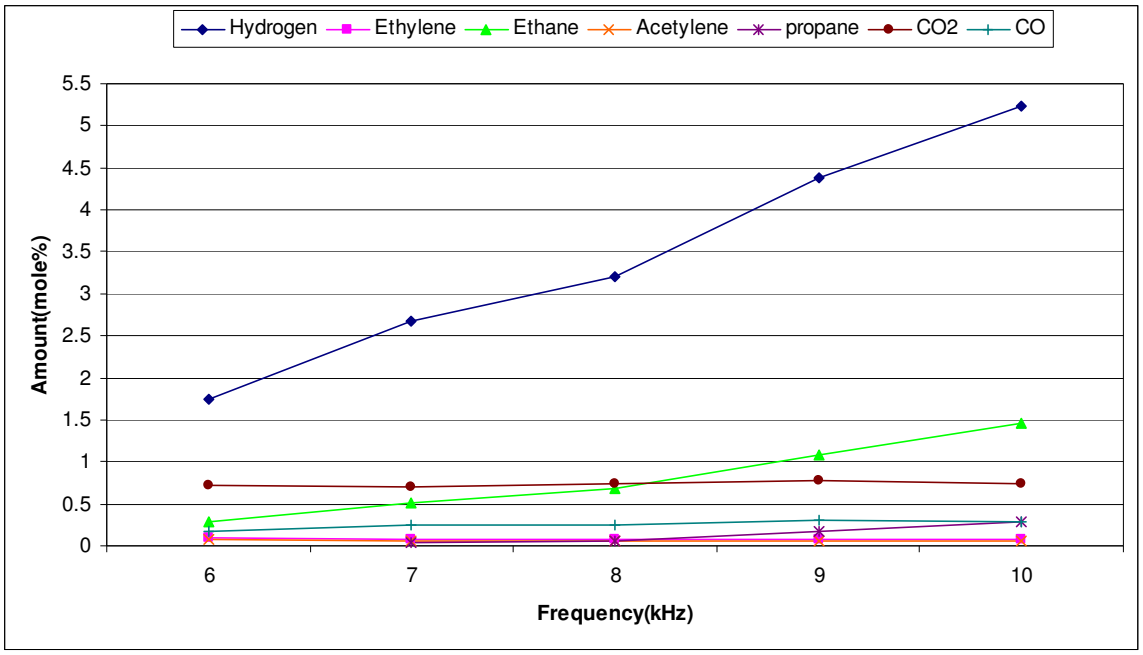

Figure 4. 3 Plot for frequency vs species amount (mol%) for methane + air (5%) mixture

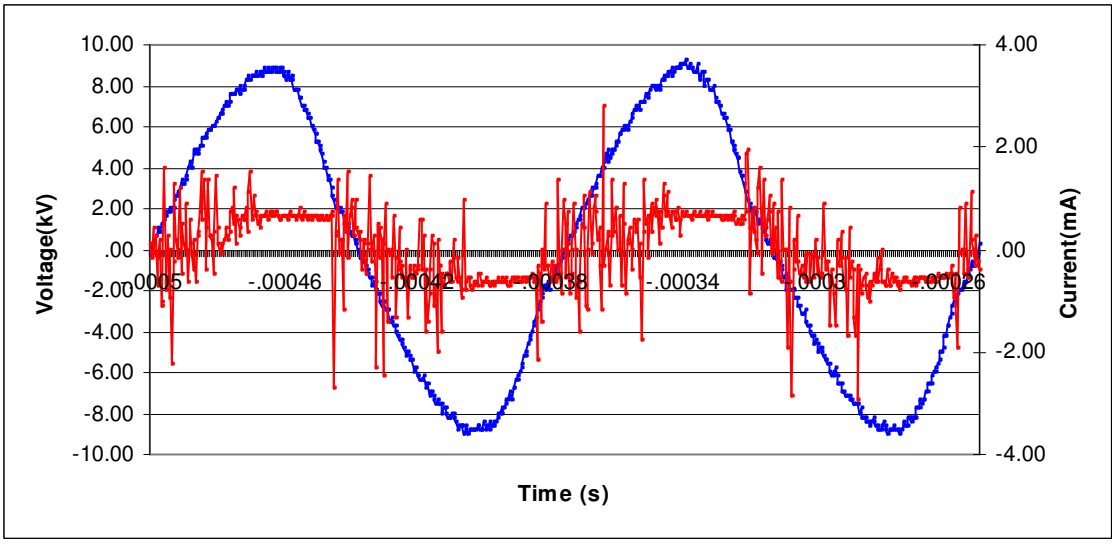

Figure 4. 4 Voltage and current waveform for methane + air (5%) at 9 kV, 8 kHz frequency

4.3 Dielectric barrier discharge in methane and air (10%) mixture

In this experimental setup, we changed the air flow rate to 0.19 L/min, which is 10% of the air flow rate we used for stoichiometric A/F ratio calculation. The methane

flow rate was maintained at 0.2152 L/min. The breakdown voltage was found to be 21 kV peak to peak at 6 kHz frequency.

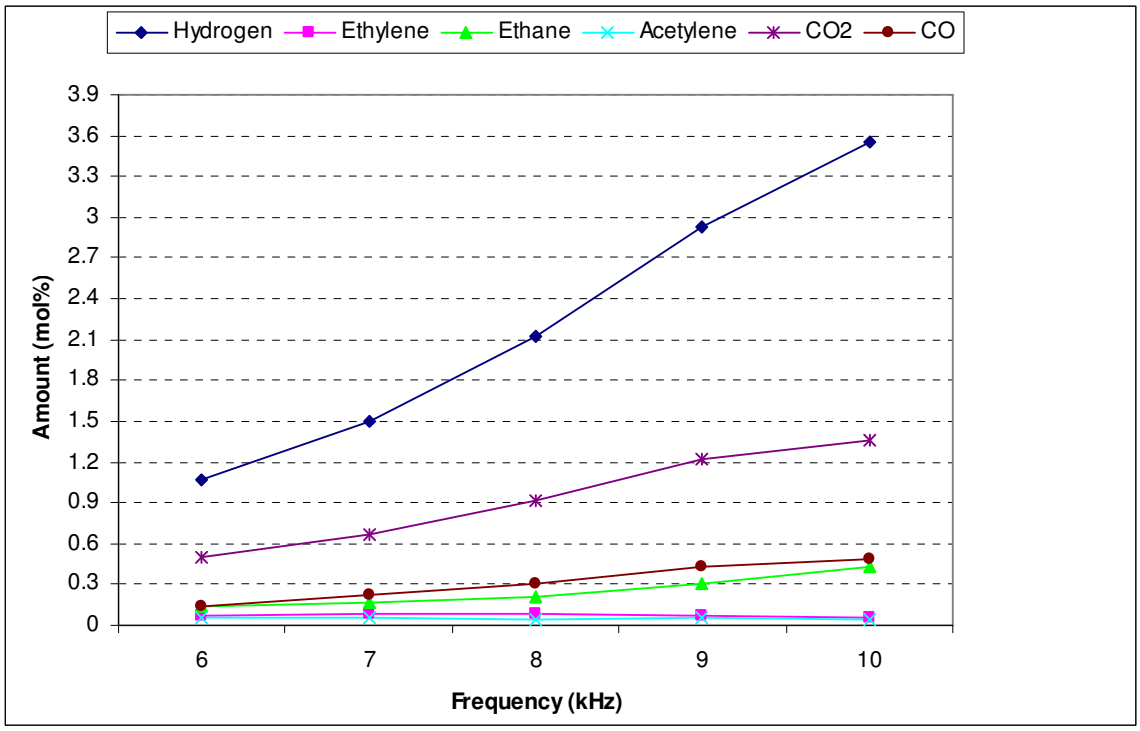

Figure 4. 5 Plot for species amount (mol%) vs frequency for methane + air (10%) mixture

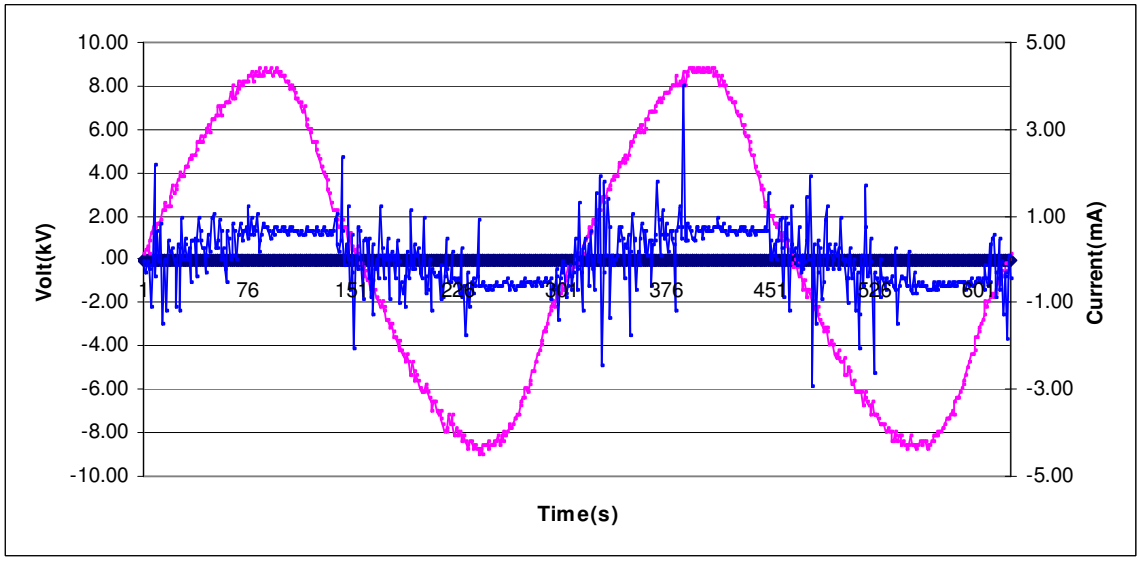

Figure 4. 6 Voltage and current waveform for methane + air (10%) at 9 kV, 8 kHz frequency

4.4 Dielectric barrier discharge in propane

Same experimental setup was used for propane gas. The flow rate used throughout the experiment was 0.09 L/min. This flow rate was based on the stoichiometriy. Before starting the experiment, we flushed the reaction chamber with the propane gas to clean the chamber. The breakdown voltage to ionize the propane gas between the electrodes was found to be 22 kV peak to peak at 7 kHz frequency. The electrodes are separated by a distance of 3mm throughout the experiment. The first set of reading was recorded at 9kv and 7 kHz using gas chromatography and the oscilloscope. The other sets of data were recorded by changing the frequency with interval 1 kHz and applying constant voltage. The effect of increasing frequency on the propane fuel is shown in Fig. 4.7 and 4.8.

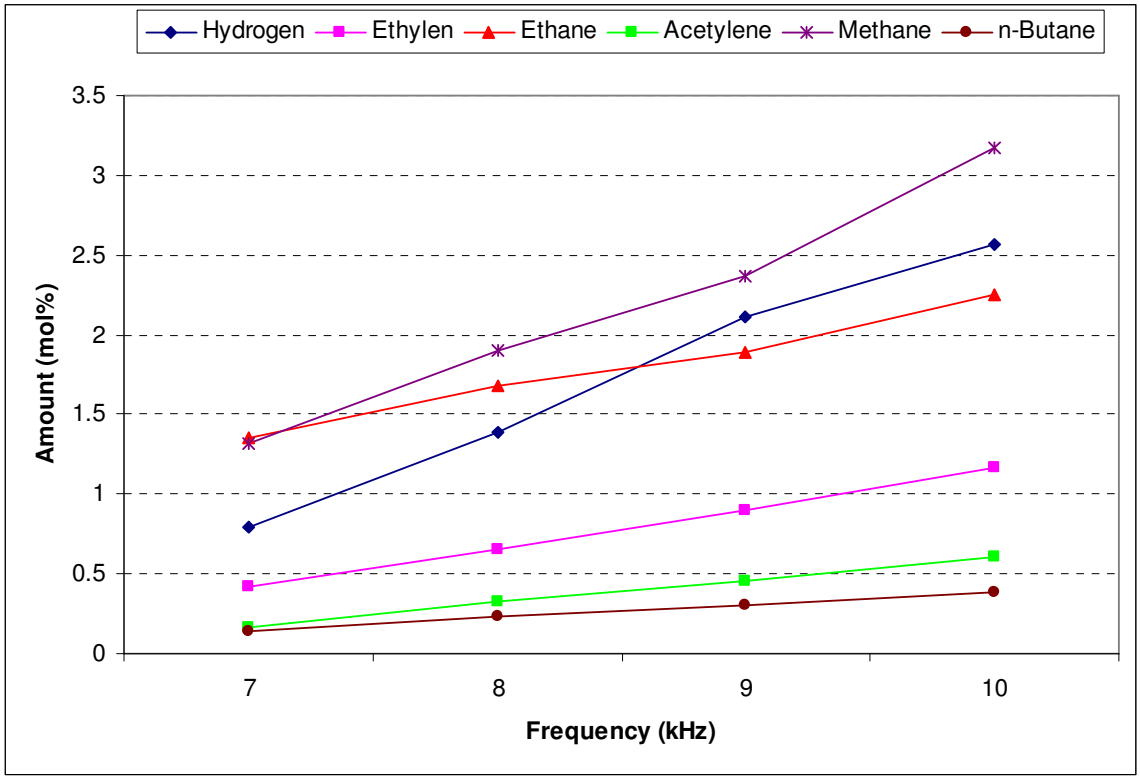

Figure 4. 7 Plot for species amount (mol% vs frequency for propane)

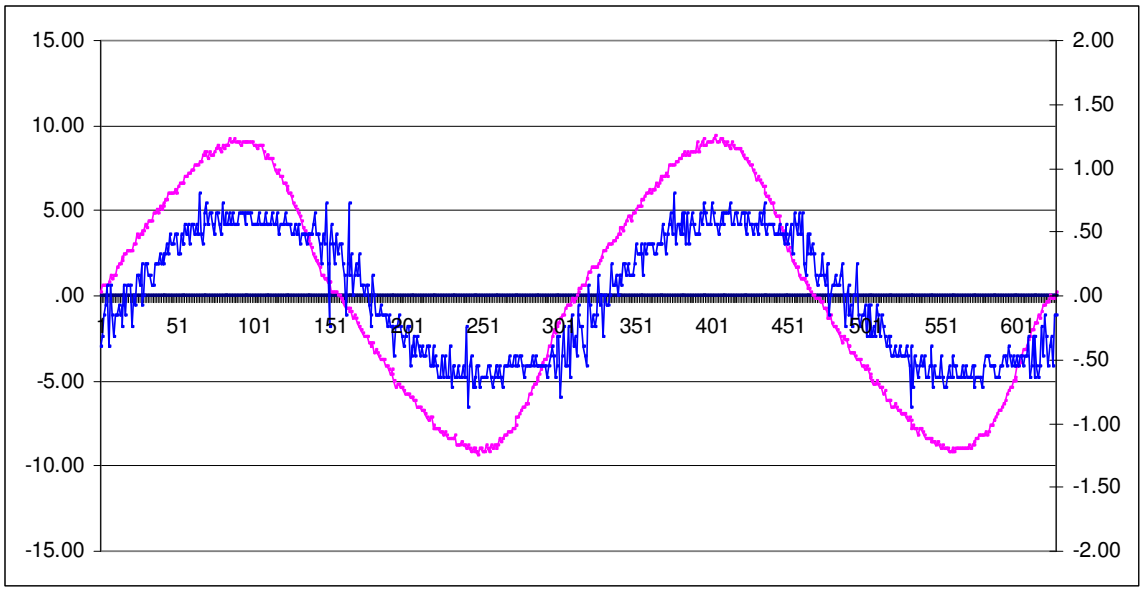

Figure 4. 8 Voltage and current waveform for propane at 9 kV, 8 kHz frequency

4.5 Dielectric barrier discharge in propane+ air (5%) mixture

The experimental setup is subjected to new air flow rate. The propane flow rate is kept constant at 0.09 l/min and air flow rate was 0.11 L/min. which is 5% of air flow rate used to calculate stoichimetric (A/F) ratio. The breakdown voltage was found to be 23 kV peak to peak at 7 kHz frequency. The mol% readings for each species were collected at different frequencies and at constant voltage using gas chromatography. The applied voltage of the system and voltage drop across the resistor was monitored using the digital oscilloscope.

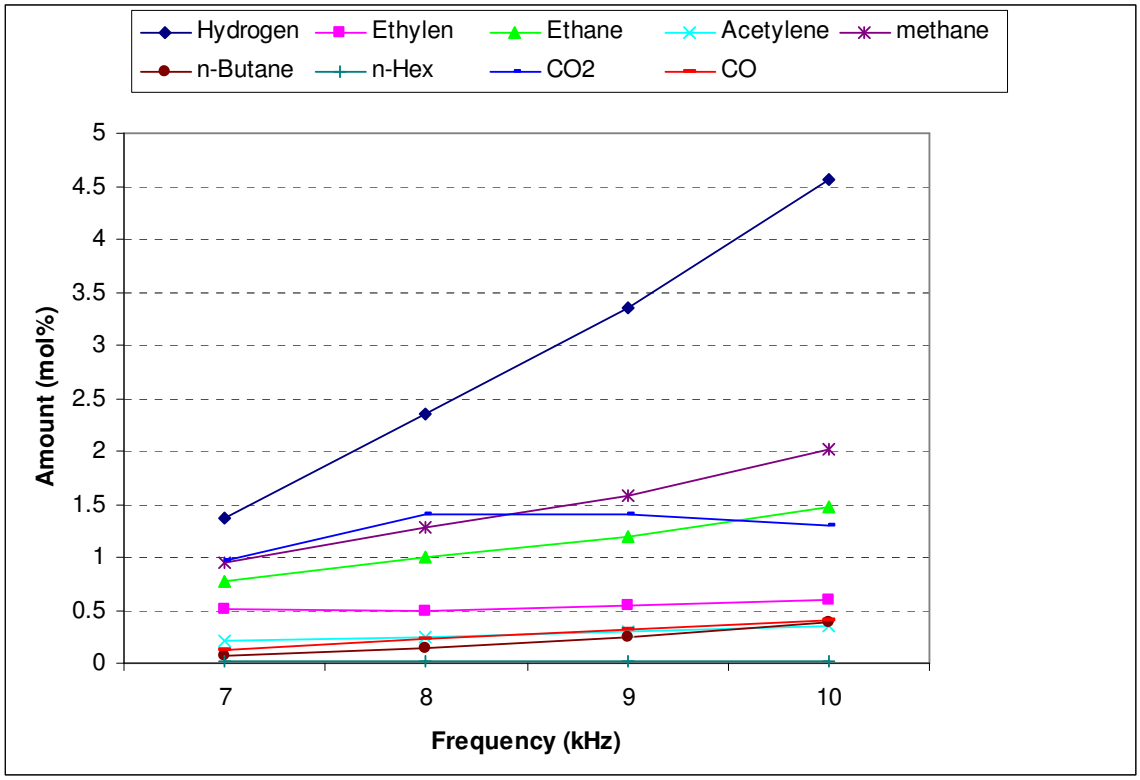

Figure 4. 9 Plot for species amount (mol%) vs frequency in mixture of propane + air (5%) mixture

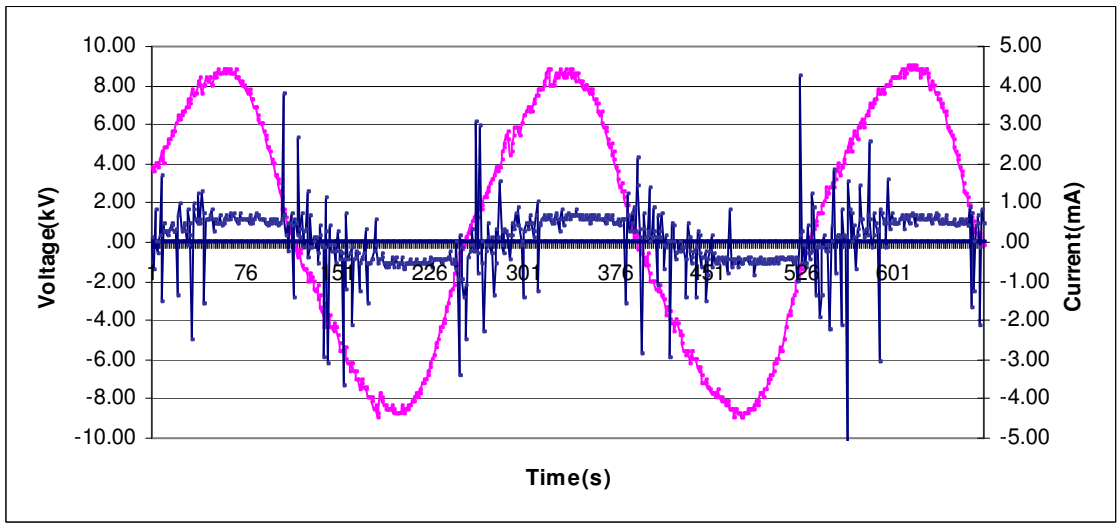

Figure 4. 10 Plot for voltage and current waveform at 9 kV, 9 kHz for propane + air (5%)

4.6 Dielectric barrier discharge in propane and air (10%) mixture

The Propane flow rate was constantly maintained at 0.09 L/min. The air flow rate increased to the 0.218 L/min, which is 10% of air flow rate used for stoichiometric (A/F) ratio calculation. The breakdown voltage was found to be 23 kV peak to peak at 7 kHz frequency. The results are shown in Figs. 4.11 and 4.12.

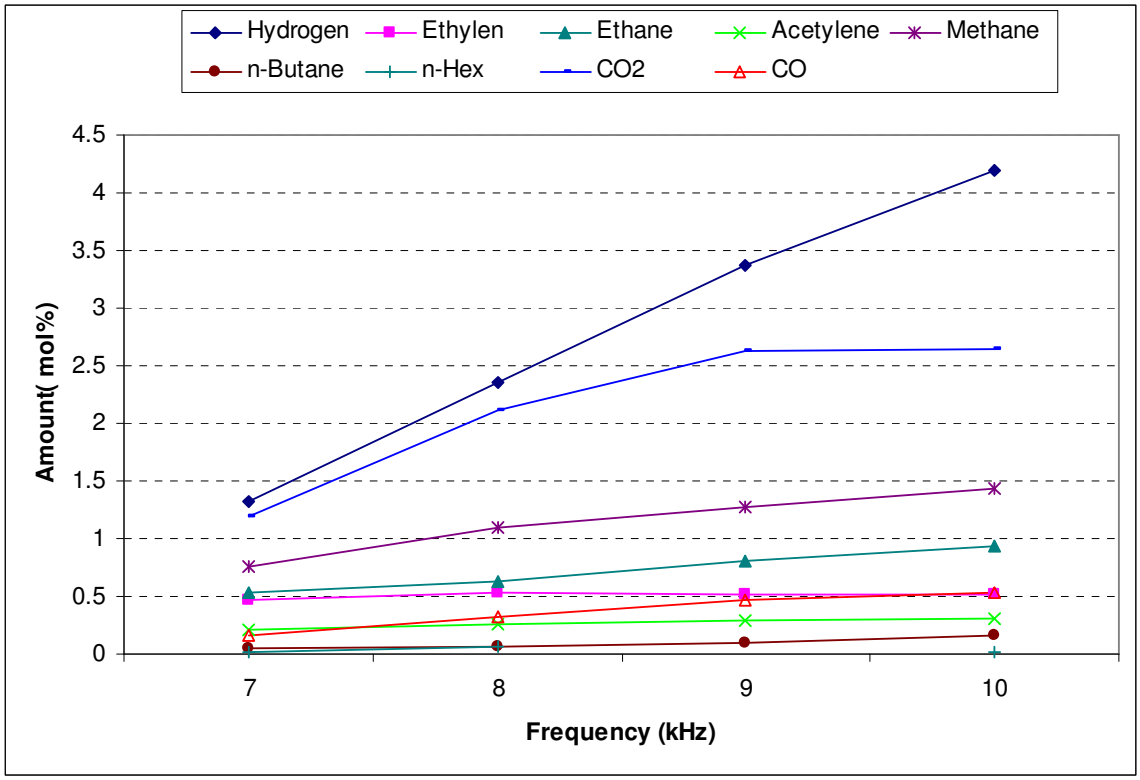

Figure 4. 11 Plot for species amount (mol%) at different frequency in the mixture of propane + air (10%)

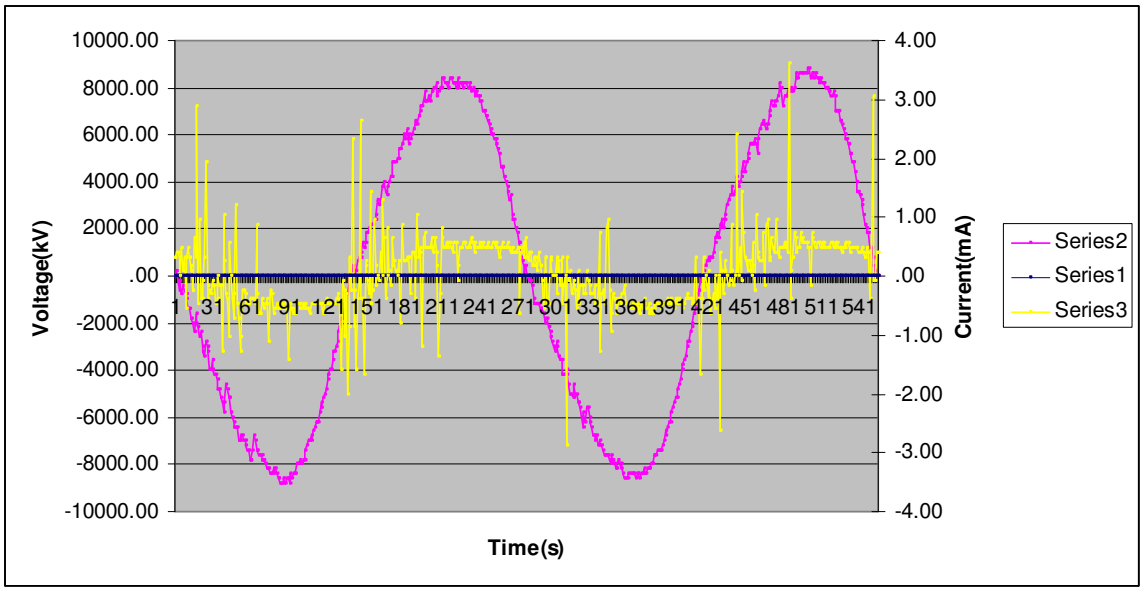

Figure 4. 12 Plot for voltage and current waveform at 9 kV, 9 kHz for propane + air (10%) mixture

4.7 Photographs of DBD

Figure 4.13-4.18 shows photographs of discharges in different mixtures with 3 mm discharge gap. The mixtures were as follows

1. Pure methane at 9kV, 6kHz
2. Methane +air 5% at 9kV, 6kHz
3. Methane +air 10% at 9kV, 6kHz
4. Propane at 9kV, 7kHz
5. Propane +air5% at 9kV, 7kHz
6. Propane +air 10% at 9kV, 7kHz

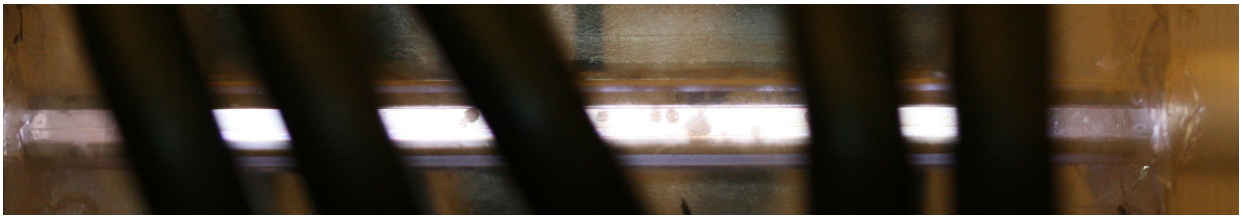

Figure 4. 13 Photograph of plasma in methane at 9 kV, 6 kHz frequency

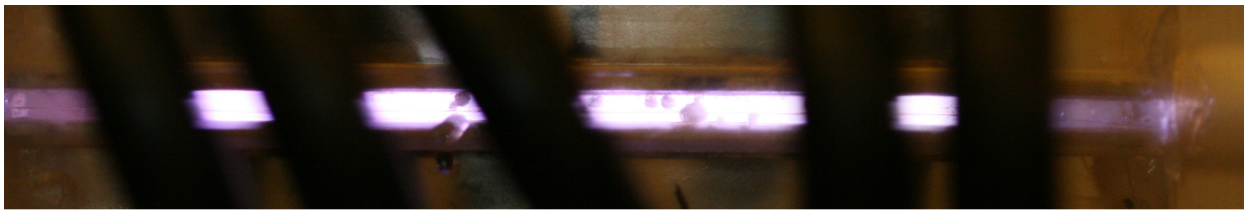

Figure 4. 14 Photograph of plasma in methane + air 5% at 9 kV, 6 kHz frequency

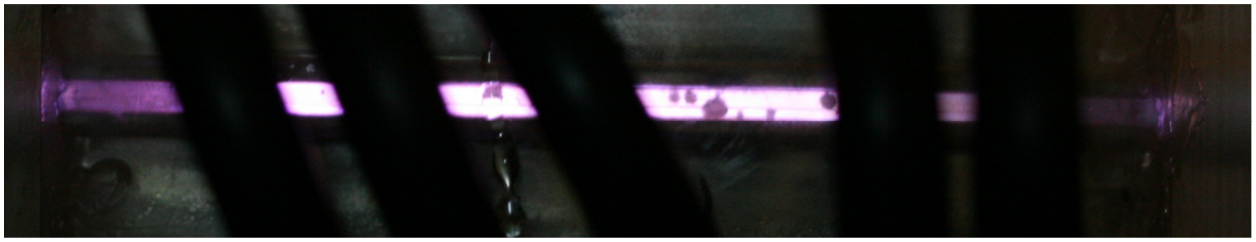

Figure 4. 15 Photograph of plasma in methane + air 10% at 9 kV, 6 kHz frequency

Figure 4. 16 Photograph of plasma in propane at 9 kV, 7 kHz frequency

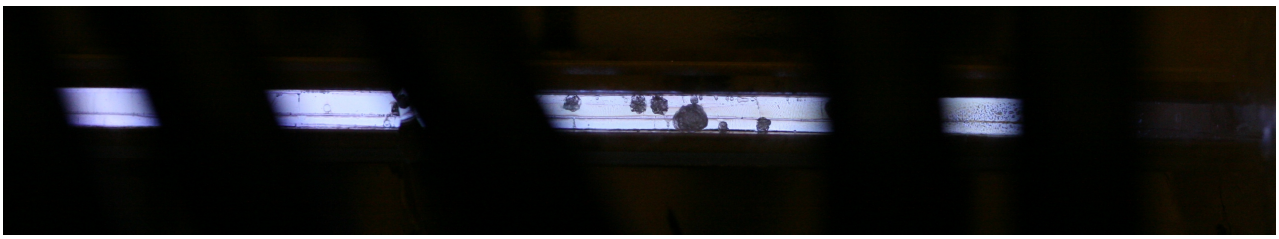

Figure 4. 17 Photograph of plasma in propane + air 5% at 9 kV, 7 kHz frequency

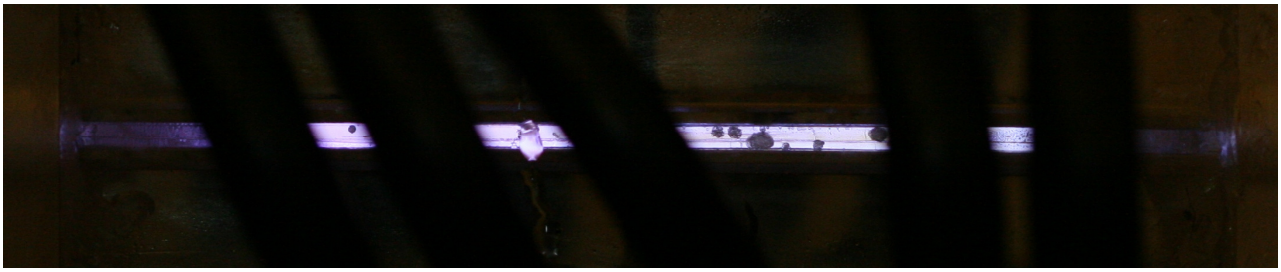

Figure 4. 18 Photograph of plasma in propane + air 10% at 9 kV 7 kHz frequency

4.8 DBD effect on the flame

Following images show the effect of plasma on methane and propane flame at different (A/F) ratios.

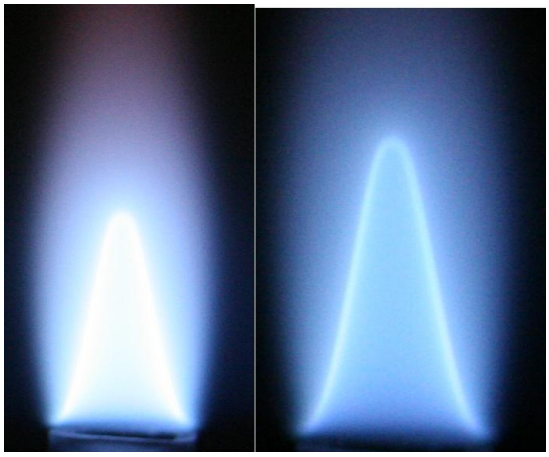

A B

Figure 4. 19 A) Lean methane flame with plasma, B) Lean methane flame without plasma at 21 kV, 8 kHz frequency

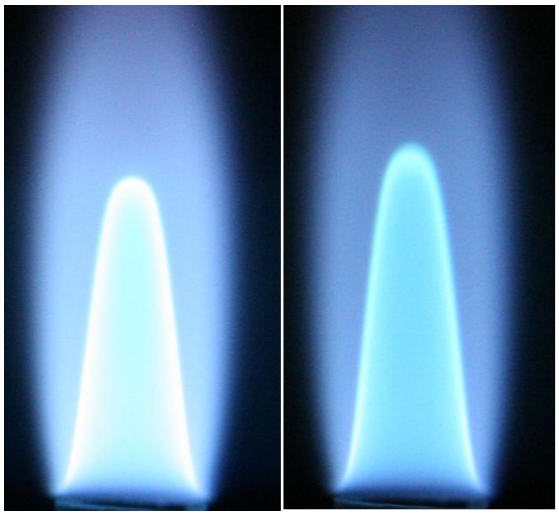

A1 B1

Figure 4. 20 A1) Rich methane flame with plasma, B1) Rich methane flame without plasma at 21 kV, 8 kHz frequency

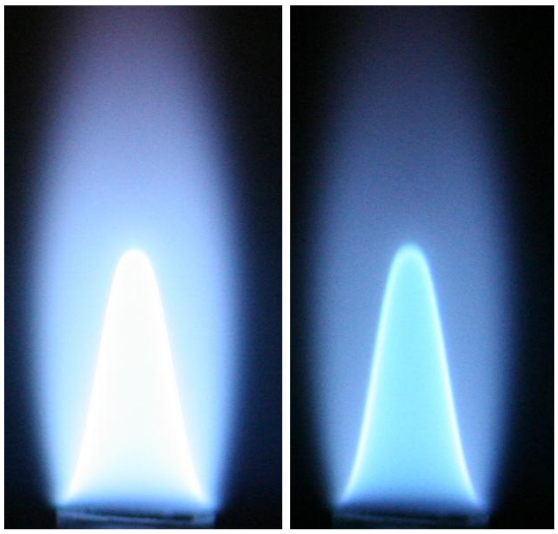

A2 B2

Figure 4. 21 A2) Stoichiometric methane flame with plasma, B2) Stoichiometric methane flame without plasma at 21 kV, 8 kHz frequency

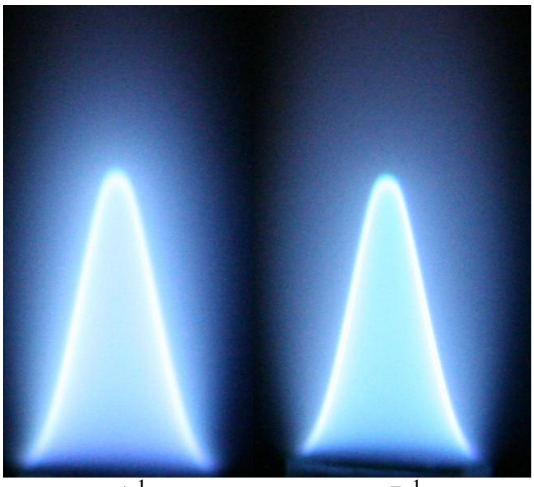

A^1 B^1

Figure 4. 22 A^1) Lean propane flame with plasma, B^1) Lean propane flame without plasma at 25 kV, 9 kHz frequency

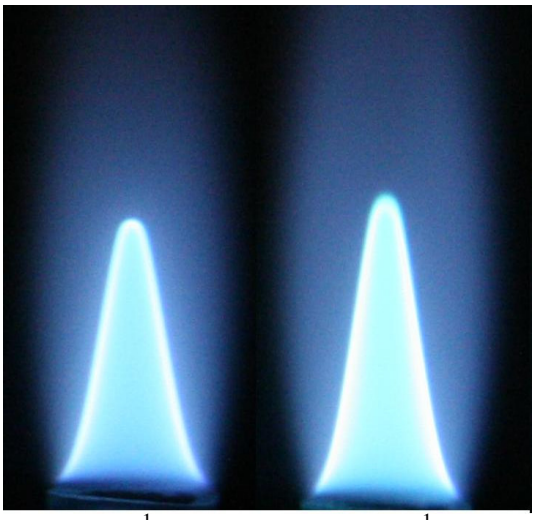

$A1^1$ $B1^1$

Figure 4. 23 $A1^1$) Rich propane flame with plasma, $B1^1$) Rich propane flame without plasma at 25 kV, 9 kHz frequency

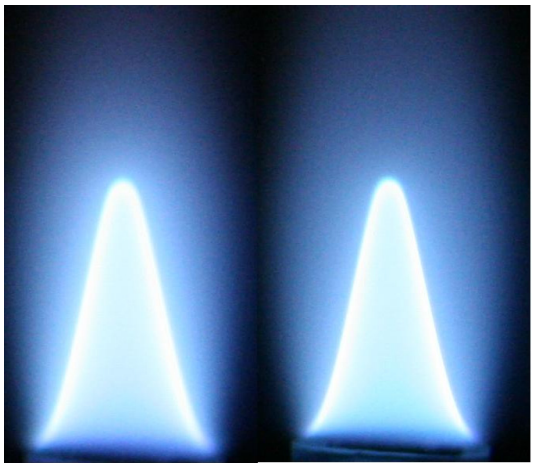

$A2^1$ $B2^1$

Figure 4. 24 $A2^1$) Stoichiometric propane flame with plasma, $B2^1$) Stoichiometric propane flame without plasma at 25 kV, 9 kHz frequency

Chapter 5 DISCUSSION

Figure 4.1 shows the effect of DBD frequency in pure methane gas. As we can see from the graph, different species are produced because of breakdown of carbon and hydrogen bonds in methane. One objective of this experiment was to produce more hydrogen by breaking carbon-hydrogen covalent bond using DBD at atmospheric pressure. The experimental results shown in Fig 4.1 strongly indicate that an increase in frequency of DBD at constant voltage increases the hydrogen production significantly. The second highest concentration product is ethane followed by propane. The reason behind that is direct conversion of methane into methyl radical by collision with electrons. The possible chemical reaction occurring between the free radicals is as follows:

$$CH_4 \rightarrow CH_3\bullet + \bullet H$$

$$CH_3\bullet + \bullet CH_3 \rightarrow C_2H_6$$

or

$$2CH_4 \rightarrow C_2H_6 + H_2$$

The direct conversion of methane into CH_2 and CH was less because the production of C_2H_2 is very small during the reaction as compared to the C_2H_6 and C_3H_8. The propane molecule concentration increases because of collision between methyl radical and ethyl radical (C_2H_5).

$$C_2H_6 + H \rightarrow C_2H_5\bullet + H_2$$

$$CH_3\bullet + C_2H_5\bullet \rightarrow C_3H_8$$

The experimental results in Fig 4.1 show increase in acetylene concentration as compared to ethylene after 8 kHz. It proves that acetylene conversion depends on pulse frequency, which means an increase in power increases acetylene production:

$$H + C_2H_6 \rightarrow C_2H_5 + H_2$$

$$H + C_2H_5 \rightarrow C_2H_4 + H_2$$

The formation of acetylene can be explained by following reactions:

$$CH\bullet + C_2H_4 \rightarrow C_2H_2 + CH_3\bullet$$

$$CH + CH \rightarrow C_2H_2$$

The production of n-butane is close to zero in the process.

Figure 4.3 shows the effect of increase in DBD frequency on the mixture of methane and air (5%). The graph shows increase in amounts of different species formation in the presence of oxygen. The rise in hydrogen production as compared to pure methane is observed after 8 kHz. It also shows the presence of CO and CO_2 in the reaction because of reactions:

$$CH_4 \rightarrow CH_3\bullet + \bullet H$$

$$CH_3\bullet + \bullet CH_3 \rightarrow C_2H_6$$

$$2\ C_2H_6 + 7\ O_2 \rightarrow 4\ CO_2 + 6\ H_2O + 1561\ kJ/mol$$

The heat released during reaction increases the temperature of the reaction chamber.

As we increase the percentage of air in mixture from 5% to 10% as shown in Fig.4.5, there is a significant decrease in the production of hydrogen and ethane, and a slight increment in CO_2 production as compared to 5% air mixture in methane. The increase in production of and CO_2 indicates that complete combustion is done in the presence of more oxygen in the mixture.

$$CH_4 + O_2 \rightarrow CO + H_2 + H_2O$$

$$CH_4(g) + 2O_2(g) \rightarrow CO_2(g) + 2H_2O(g) - 890kJ/mol$$

$$2\ C_2H_6 + 7\ O_2 \rightarrow 4\ CO_2 + 6\ H_2O + 1561\ kJ/mol$$

$$2\ CH_4 + O_2 \rightarrow 2\ CO + 4\ H_2$$

Use of air increases the formation of species in the reaction, which is confirmed by measuring the species concentrations in pure methane, 5% air methane, and 10% air methane. Figure 5.1 shows the trend of increase in hydrogen concentration in 5% air as compared to pure methane and 10% air, from 9 kHz frequency.

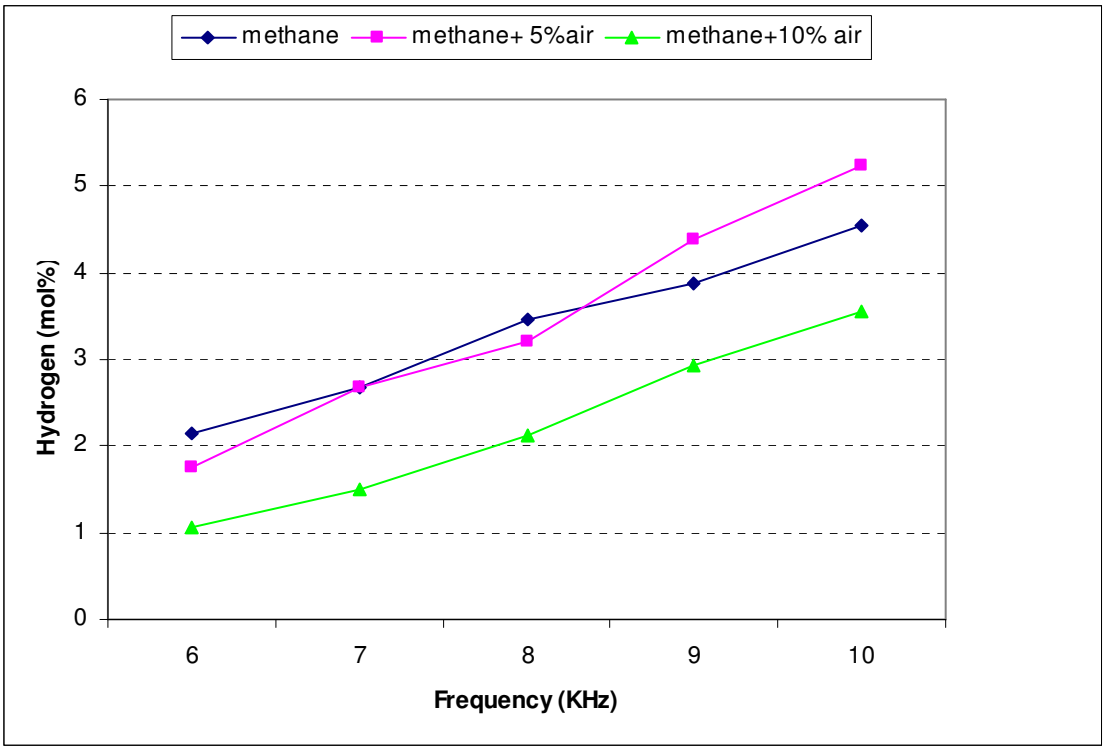

Figure 5. 1 Comparison of hydrogen production in different air mixture

Figure 5.2 shows the highest production of ethane in pure methane when compared to 5% air and 10% air. The graph shows the increment in the ethane as compared to 10% air with increase in the frequency after 8 kHz. The reason for this behavior is excitation of oxygen atom and increase in number of high energy electrons.

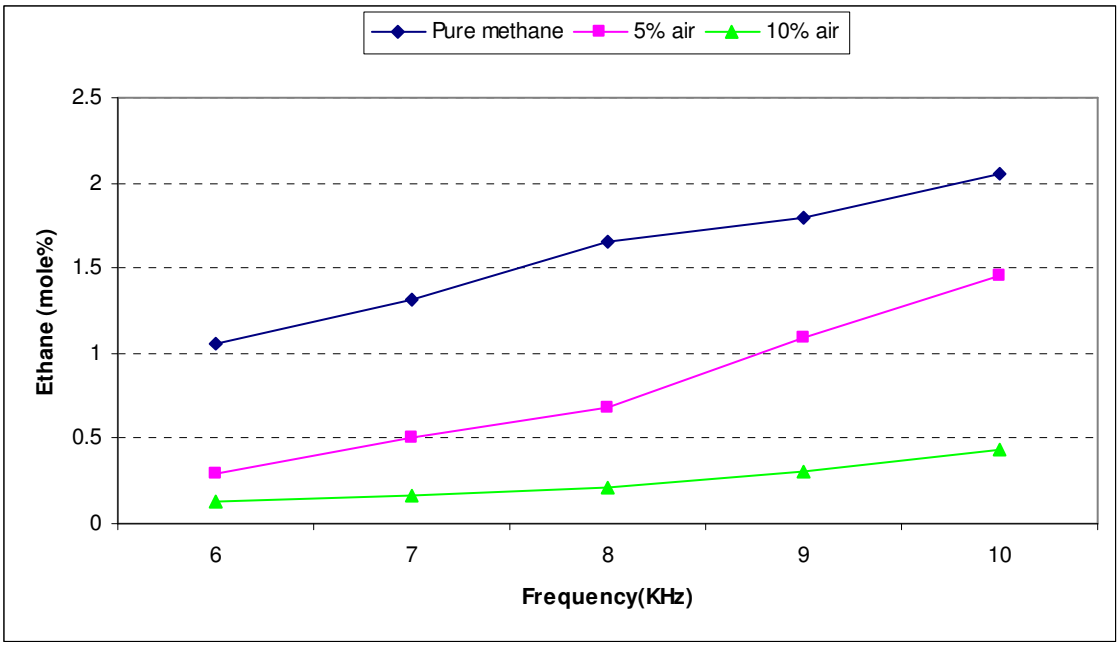

Figure 5. 2 Comparison of C_2H_4 production in different air mixture

Figure 5.3 shows the comparison of ethylene and acetylene in methane and different mixture of air (5% and 10%).It shows that there is no improvement in production of C_2H_4 and C_2H_2 as compared to pure methane. It also shows with the increase in frequency decreases the production of C2H4 and C2H2 in air mixture.

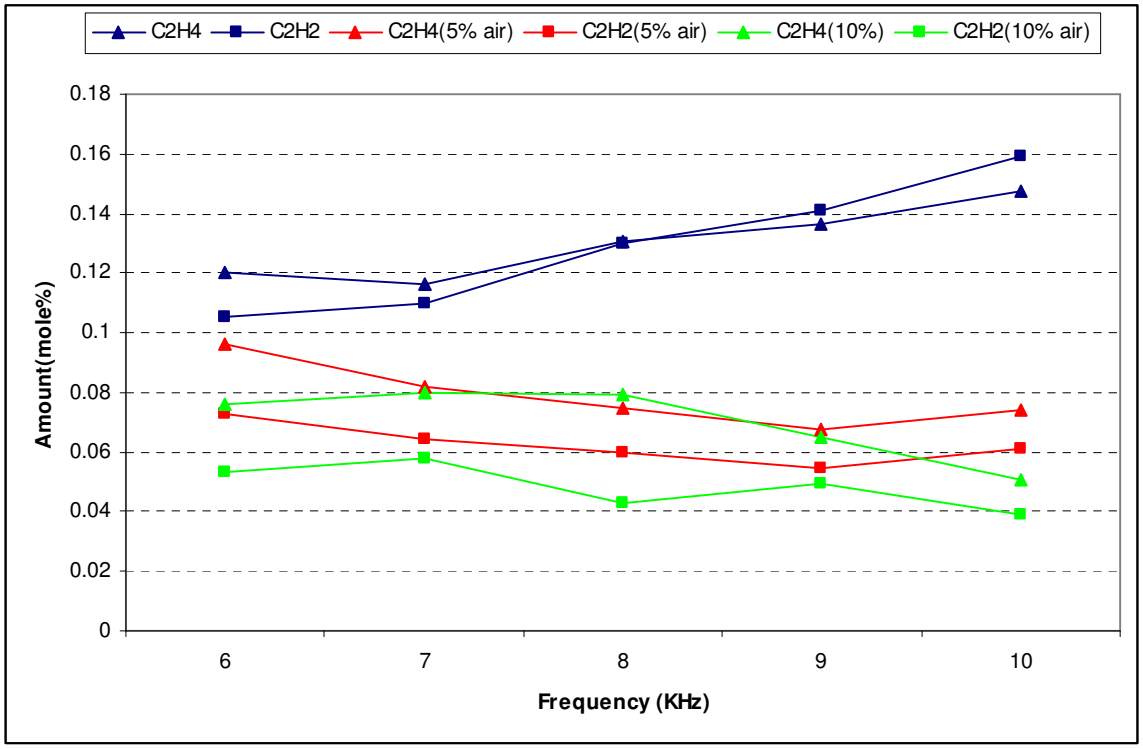

Figure 5. 3 Comparison of C_2H_4 and C_2H_2 in different air mixture

Figure 5.4 shows production of CO and CO_2, which are observed in the presence of oxygen. In 10% air the production rates of CO and CO_2 are high because of the high percentage of oxygen available in the mixture. The difference between the concentrations of CO_2 and CO is higher in 10% air than in 5% air. This indicates that more CO is reacting with oxygen atom and forming CO_2.

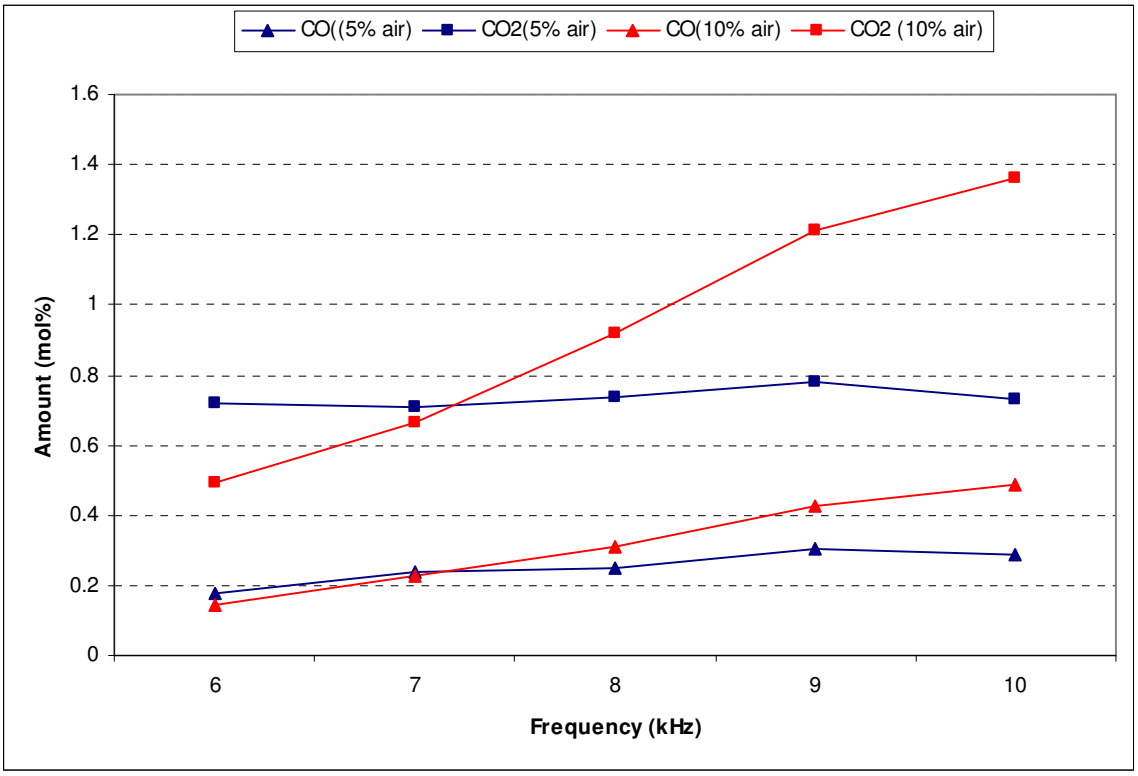

Figure 5. 4 Comparison of CO and CO_2 production in 5% and 10% air in methane

Figure 4.7 shows the effect of DBD frequency on propane. It is observed that with the increase in frequency, the mole concentrations of the products increase. The first product of propane decomposition is methane and then hydrogen, ethane, ethylene, acetylene, n-butane. Based on these results, following chemical reactions are proposed:

$$e + C_3H_8 \rightarrow C_2H_5 \bullet + CH_3 \bullet + e$$

$$e + C_3H_8 \rightarrow 2CH_3 \bullet + CH_2 : + e$$

$$e + C_3H_8 \rightarrow C_3H_7 \bullet + H\bullet + e$$

Methane production can be explain by the following reaction:

$$C_3H_8 \rightarrow 2H_2 + CH_4 + 2C$$

At low frequency, production of hydrogen is less than that of ethane, which is explained by less number of collisions between high energy electron and ethane molecule. As we increase the frequency to 9 kHz and above, the production of hydrogen and methane increases because the higher frequency increases the possibility of collision between electron and molecule by proceeding further decay of decomposition product. This is explained by following reactions:

$$H\bullet + C_2H_5\bullet \rightarrow 2CH_3\bullet$$

$$CH_3\bullet + CH_3\bullet \rightarrow C_2H_6$$

$$e + C_2H_6 \rightarrow CH\bullet + CH_3\bullet + H_2 + e$$

$$e + C_2H_6 \rightarrow C_2H_4^* + H_2 + e$$

$$H\bullet + C_2H_6 \rightarrow C_2H_5\bullet + H_2 \text{ or } CH_3\bullet + CH_4$$

$$CH\bullet + C_2H_6 \rightarrow C_2H_2 + CH_4 + H\bullet$$

$$CH2: + C_3H_8 \rightarrow \text{n/iso-}C_4H_{10}$$

Figure 4.7 indicates that a major part of applied energy is utilized to decompose propane into hydrogen, methane and ethane.

Figure 4.9 shows the effect of increasing frequency on the mixture of propane and air (5%). The graph indicates the increase in hydrogen mole concentration in the presence of 5% air as compared to pure methane conversion. It also shows increase in number of species such as CO of CO_2 and n-Hexane. The formation of n-Hexane and ethylene does not show any effect of increase in frequency. Based on these results, following reactions are proposed:

$$C_3H_8 \rightarrow 2H_2 + CH_4 + 2C$$

Complete combustion of propane.

$$C_3H_8 + 5\ O_2 \rightarrow 3\ CO_2 + 4\ H_2O + heat$$

Partial oxidation of methane

$$2\ CH_4 + O_2 \rightarrow 2CO + 4H_2$$

$$2\ CH_4 + H2O \rightarrow CO + 3H_2$$

It also produces ozone (O_3) which we did not measure during the experiments:

$$O + O_2 \rightarrow O_3$$

$$O_3 \rightarrow O + O_2$$

Formation of CH_4, C_2H_6, and C_2H_2 is a result of hydrogenation and dehydrogenation of exited radical and collision between electrons and molecules.

As shown in Fig.4.11, with the increase in the flow rate of air in the propane, the production of hydrogen does not show any change as compared to the 5% air. A small increment observed at 10 kHz frequency. The CO_2 shows noticeable change in the production. This indicates that high concentrations of O_2 efficiently convert maximum amounts of carbon into CO_2 and produce H_2O in complete combustion processes. The graph shows CO_2 at its max, at 8 kHz & 9 kHz. Ethylene, acetylene and n-Hexane do not show any effect of increasing frequency on the production. The following reactions are proposes based on the results:

$$HCHO + O \rightarrow HCO + OH$$

$$HCO + O \rightarrow CO + OH$$

$$HCO + O \rightarrow CO2 + H$$

$$HCO + H \rightarrow CO + H_2$$

Figure 5.5 shows the growth of hydrogen formation in 5% air with respect to pure propane. There is no considerable growth found in the 10% air with respect to 5% air up

till 9 kHz frequency. It means that high power is required for a higher flow rate of air to produce more active species.

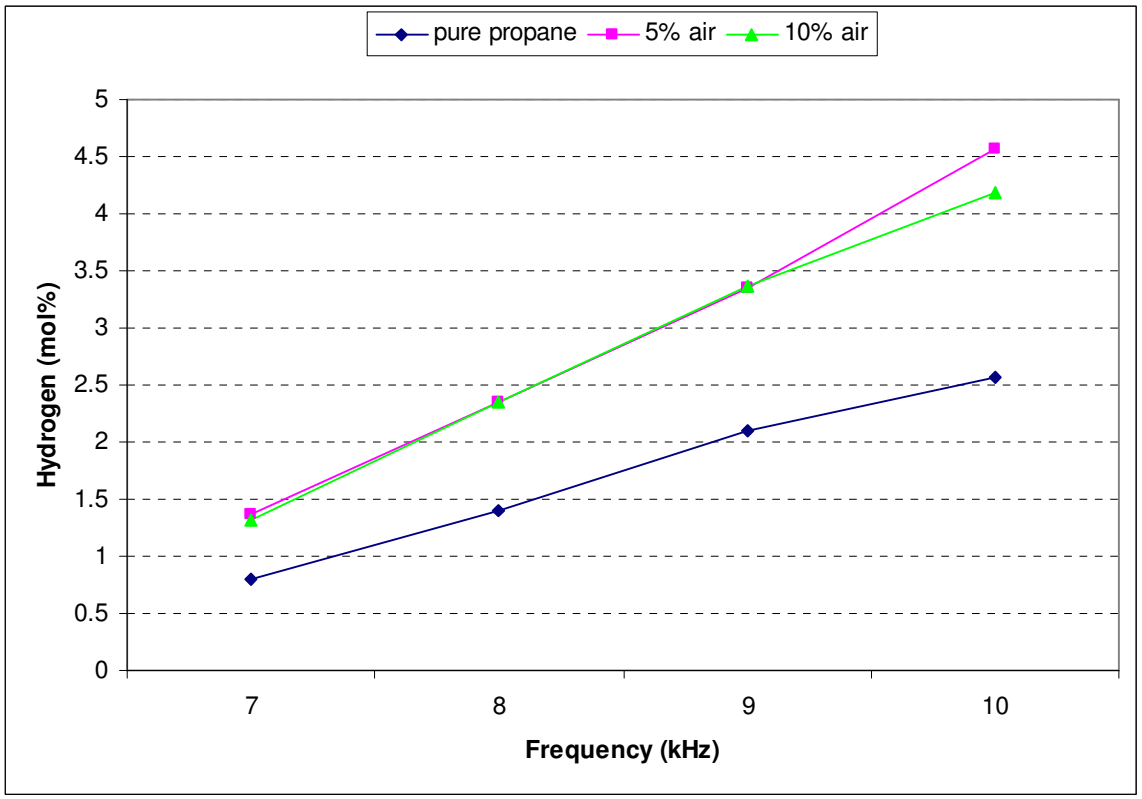

Figure 5. 5 Comparison of H_2 species formation in the methane, 5% air and 10% air mixture

Figure 5.6 shows decrease in CH_4 production, as we increase the air concentration. Most of the ethane molecule is converting into ethyl radical and hydrogen atom instead of methyl radical and methane. This is supported by Figure 5.5 where hydrogen concentration is higher in 5% air and 10% air as compared to pure propane.

The reaction path is as follows:

$$H\bullet + C_2H_6 \rightarrow C_2H_5\bullet + H_2$$

$$H\bullet + C_2H_6 \rightarrow CH_3\bullet + CH_4$$

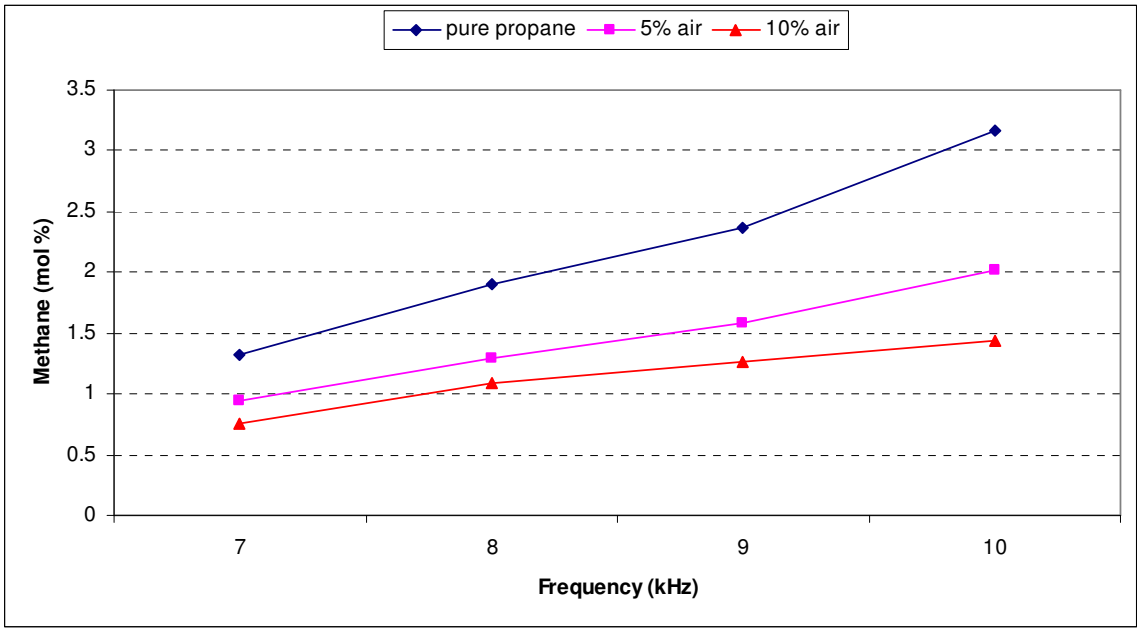

Figure 5. 6 Comparison of CH_4 species formation propane, 5% air and 10% air mixture

Figure 5.7 shows the production of CO and CO_2 in propane-5% air and propane-10% air mixtures. The production of these species occurs due to the oxygen molecule. The graph indicates that the increase in oxygen concentration increases the combustion rate of the hydrocarbons species. It also increases the reaction rate of C and CO with the O_2 and O radicals. That may be one of the reasons of lower concentration of CO as compared to CO_2 in 10% air mixture. The concentration of CO_2 can be seen at its max in 9 kHz and 10 kHz frequency in 10% air mixture.

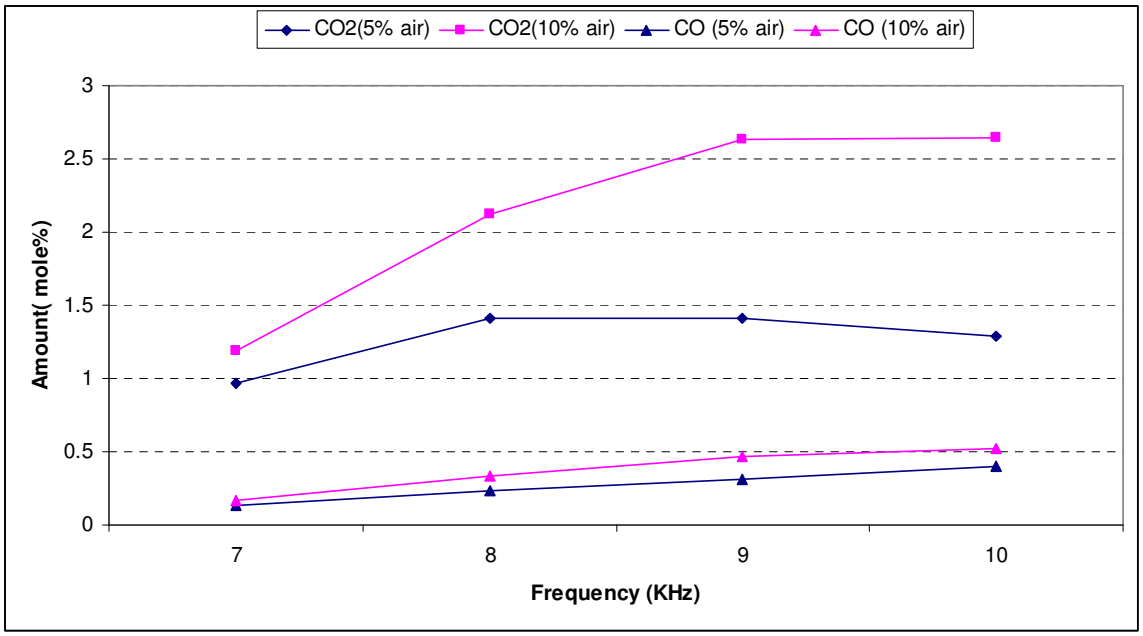

Figure 5. 7 Comparison of CO_2 and CO species formation in propane, 5% air and 10% air mixture

Figure 5.8 shows the trend of C_2H_4 and C_2H_6 decreasing with addition of 5% air and 10% air. There is not any noticeable difference in the production of C_2H_4 with respect to increase in air. It means that there was less dehydrogenation of C_2H_6 radicals. In the beginning, most of electron energy gets absorbed in the activation of O_2 molecule. This reduces the possibility of collision between electron and molecules, radicals and neutral species.

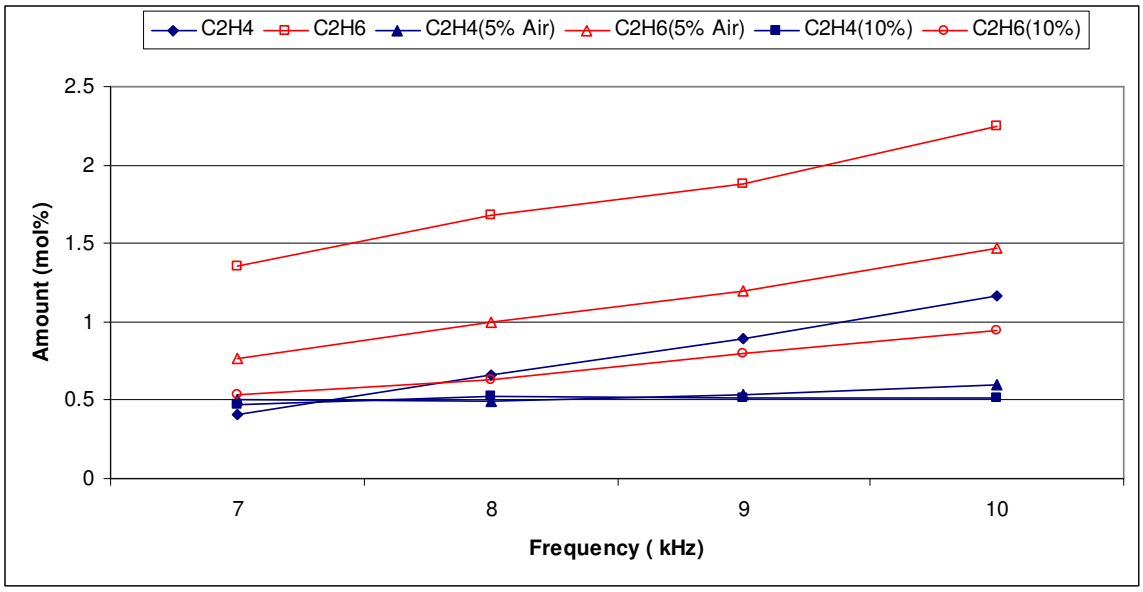

Figure 5. 8 Comparison of C_2H_4, C_2H_6 species formation in the propane, 5% air and 10% air mixture

The photographs of discharges generated during the experiments in methane and propane at different concentrations (5%, 10%) of air are shown in Figs. 4.13 - 4.18. The discharge generated is filamentary in the nature (this is proved from each voltage and current plot) and has purple color in methane and milky white in propane. The discharge is uniform, and is completely developed all over the electrode surface area.

Figure 4.19 - 4.21 show the effect of plasma on methane flame at lean, rich and stoichiometric (A/F) ratios. At lean (A/F) ratio, plasma shows effect on combustion by decreasing the length and size of the flame. In the rich air-fuel ratio, it also decreases in the flame length. There is no plasma effect observed on the flame length at stochiometric (A/F) ratio.

The effect of plasma on the propane flame at different (A/F) ratios is shown in Figs. 4.22 - 4.24. The visual observations indicate that in lean propane flame, the outer diffusive flame area decreasing under the effect of plasma. In rich (A/F) ratio (Fig. 4.23),

plasma shows noticeable change in the flame dimensions ($A1^1$) as compared to the non plasma flame ($B1^1$). Fig. 4.24 shows no effect of plasma on the stochiometric (A/F) ratio.

Chapter 6 SUMMARY

The current work deals with reforming of methane and propane into easier combustible lower hydrocarbons with the help of dielectric barrier discharge (DBD) at atmospheric pressure and room temperature. Two electrode assemblies, which include a dielectric plate attached to the electrode, were used to generate discharge by applying ac voltage. The reaction chamber with a cooling system was designed to perform the experiments.

The following effects were studied:

- Effect of DBD on methane.
- Effect of DBD on the mixture of methane and 5% air.
- Effect of DBD on the mixture of methane and 10% air.
- Effect of DBD on propane.
- Effect of DBD on the mixture of propane and 5% air.
- Effect of DBD on the mixture of propane and 10% air.

The first three sets were performed at 9 kV constant voltage over the frequency range from 6 to 10 kHz. The methane flow rate was maintained at 0.2152 L/min, while the air flow rate was 0.095 L/min for 5%air and 0.19L/min for 10%air in the mixture. The breakdown voltage for methane was 21 kV peak-to-peak. The experimental results show successful decomposition of methane into hydrogen and other higher hydrocarbon (C_2H_4, C_2H_6, C_3H_8, C_2H_2) gases. Addition of 5% air showed an increment in hydrogen production at 9 kHz and 10 kHz. CO and CO_2 formed in the presence of air, and their concentrations were found to be higher in 10% air than in 5% air. This indicates that excess amount of oxygen in plasma helps complete combustion.

The propane sets of experiments were performed at 9 kV, at frequency varying from 7 kHz to 10 kHz. The breakdown voltage was 22 kV peak-to-peak. The fuel flow rate (0.091 L/min) and distance (3 mm) between the electrodes were maintained constant throughout the experiment. The decomposition of propane shows descending order of methane, ethane and hydrogen concentrations. The production of hydrogen increased in the presence of air. Also, the formation of new species (CO, CO_2, n-hexane) was observed. It indicates that oxygen molecules help to ionize the gas by providing more number of electrons at a lower power. The mixture of propane with 10% air shows higher production of CO and CO_2 than in 5% air.

The effect of DBD on the structure of methane-air and propane-air diffusion flames was studied at different A/F ratios. For both methane and propane, it was found that plasma noticeably changes the structures of lean and rich flames.

REFERENCES

[1] R. Foest, M. Schmidt, K. Becker. International Journal of Mass Spectrometry Volume 248, Issue 3, 15 February 2006, Pages 87-102 “Micro plasma, an emerging field of low-temparature plasma” .Science and technology.

[2] R. Foest, F. Adler, F. Sigeeneger, and M. Schmidt. Surf. Coat tec 163-164, 323 (2003)

[3] Y. S. Akishev, A. A. Deryugin, I. V. Kochelov, A. P. Napartovich and N. I. Trushkin; J. phys. D. Appl. phys. 26, 1630 (1993).

[4] Y. P. Raizer, “Gas Discharge Phyiscs”, New York Springer, 1991.

[5] Valery , A. Godyok, Fellow, IEEE 2006.“ Non equilibrium EEDF in gas discharge plasmas”.

[6] F. Massines, A. Rabehi, P. Decomps, R. B. Gadri, P. Ségur, and C. Mayoux, J. Appl. Phys. 83, 2950 (1998); doi:10.1063/1.367051. “Experimental and theoretical study of a glow discharge at atmospheric pressure controlled by dielectric barrier”.

[7] C. Hudon, R. Bartnikas, and M. R. Wertheimer, IEEE Trans. Electr. Insul. 28, 1(1993).

[8] P. H. F. Morshuis, “Partial Discharge Mechanisms”, (Delft University Press, Delft, 1993).

[9] T. Yokoyama, M. Kogoma, S. Kanazawa, T. Moriwaki and S. Okazaki, J. Phys. D: 23, 874(1990).

[10] J. Stanco, T. Doerk, J. Ehlbeck, P. Jauernik, J.H. Schäfer and J. Uhlenbush, J. Phys. D26, 244 (1993).

[11] J. Zhang, J. Sun, D. Wang and X. Wang, Thin solid Films 506 – 507 (2006) 404-408.

[12] C. Schrader, L. Baars-Hibbe, K. Gerike, E. M. Veldhuizen, N. Lucas, P. Sichler and S. Büttgenbach, Science direct.com (Vacuum).

[13] L. L. Raja, X. Yuan and J. Shin, “One-dimensional simulation of multi pulse phenomena in dielectric-barrier atmospheric-pressure glow discharges,” Vacuum Tech.

[14] E. E. Kunhardt, “Generation of large volume, atmospheric-pressure, non-equilibrium plasmas,”IEEE Trans Plasma Sci. 2000; vol. 28:189.

[15] S. Kanazawa, M. Kogoma, T. Moriwaki and S. Okazaki, “Stable glow plasma at atmospheric pressure,” J. Phys. D: Phys. 21 (1988), 838-840.

[16] F. Massines, P. segur, N. Gherardi, C. Khamphan , A. Ricard.
“Physics and chemistry in a glow dielectric barrier discharge at atmospheric pressure: diagnostics and modeling”.

[17] Y. H. Choi, J.H. Kim, Y. S. Hwang. Thin solid films 506-507(2006)389-395. “One dimensional discharge simulation of nitrogen DBD atmospheric pressure plasma”.

[18] Y. s. Akishev, A.V. Dem yanov, V. B Karal’nik, M.V. Pan’kin, and N. I. Trushkin Vol. 27, NO2 pp 176-183, 2001. “pulse Regime of the Diffusive mode of a Barrier Discharge in Helium” Low temperature plasma.

[19]Y. Dan, G. Dengshan, Y. Gang, S. Xianglin and G. Fan. Journal of Hazardous Materials, B 127 (2005) 149-155.“ An investigation of the treatment of particulate matter from gasoline engine exhaust using non-thermal plasma”,

[20]A. J .Beaulieu. “Transversely excited atmospheric pressure CO2 laser,” Appl. Phys. Lett. Vol. 80, pp. 1722-1724,2002.

[21]Y. S. Akishev, A. A. Deryugin, V. B Karal’nik, I. V. Kochetov, A.P. Napartovich, and N. I. Trushkin. Plasma phys. Rep. vol20, p.511,1994. “Numarical simulation and expremental study of an atmospheric-pressure direct current glow discharge,”

[22] A Fridman, A Chirokov and A Gutsol. J. phys. D; Appl. Phys, 38(2005)R1-R24
“Non-thermal atmospheric pressure discharges”.

[23]A. Bogaerts, E. Neyts, R. Gijbels, Joost van der Mullen, spectrochimica Acta Part B57 (2002) 609-658.“Gas discharge plasmas and their applications”.

[24]H.Conrads, M.Schmidt, plasma sources Sci Technol. 9 (2000) 441-446. “Plasma generation and plasma sources”.

[25] D.Trunec, A. Brablec and J. Buchta, .” J. Phys.D: Appl Phys.34 1697-1699, 2001.
“Atmospheric pressure glow discharge in neon”.

[26] F. Massines, A. Rabehi, P. Decomps, R. B. Gadri, P. Segur, and C. Mayoux, J. Appl.Phys. Vol.83, No.6, 1998.
“Expremental and theoretical study of a glow discharge at atmospheric pressure controlled by dielectric barrier”.

[27] Y. U. B Golubovskii, V. A. Maiorov, J. Behnke and J. F. Behnke. “J. Phys. D: Appl. Phys.36(2003) 39-49. “Modeling of homogeneous barrier discharge in helium at atmospheric pressure”.

[28] P. Segar and F. Massines 2000 Proc. 13th Int. Conf. on Gas discharge and their Applications(GD 2000) (Glasgow 3-8 september 2000).

[29] Y. S. Akihev, A. V. Dem Yanov, V. B Karal'nik, M. V. Pan'kin and N. I. Trushkin 2001 Plasma phys. Rep.27 164(2001 Fizika plasmy 27 170)

[30] B. Eliasson and U. Kogelschatz, IEEE Trans. Plasma Sci. 19, 309(1991).

[31] V. G. Samoilovich, V. I. Gibalov, and K. V. Kozlov, (Mosk. Gos. Univ., Moscow, (1989). " Physical chemistry of Barrier Discharge".

[32] I. Brauer, C. Punset, H.-G. Purwins, and J. P. Boeuf, J.Appl. Phys. 85, 7569 (1999).

[33] A. D. Barkalov, V. D. Gavrilyuk, G. G. Gladush, et al., Teplofiz. Vys Temp.16, 265 (1978).

[34] F. Massines, R. Messaourdi, and C. Mayoux, plasma polym.3 (1), 43 (1998)

[35] Y. Tenzin , May 2007. Uni. Of texas at elpaso.
"Electrical and optical characteristics of dielectric barriers, microhollow cathode and hybride mode discharge at atmospheric pressure".

[36] L.B. Loeb, University of California Press, Berkeley, CA, 1965.
"Electrical Coronas: Their Basic physical Mechanism".

[37] http://en.wikipedia.org/wiki/Corona_discharge.

[38] D. D. Hsu and D. B Graves plasma chemistry and plasma processing, vol 25 No1 February 2005. "Micro hallow Cathode Discharge Reactor Chemistry".

[39] K. H. Schoenbach, Laser Processing Consortium – FEL User's Workshop, March 20, 2003.Physical Electronics Research Institute, Old Dominion University, Norfolk, VA.

[40] P. S. Kothnur, J. shin, and L. L. Raja. IEEE transactions on plasma science, vol.33, NO 2, April 2005."Experimental and Numerical Study of External Plume Characteristics in Microhollow Cathode Discharges".

[41] M. Miclea, K. Kunze, U. Heitmann, S. Florek, J. Franzke, and K. Niemax J. Phys. D: Appl. Phys., 38, 1709-1715, 2005., "Diagnostics and application of the microhollow cathode discharges as an analytical plasma".

[42] M. P. Gomes, B. N. Sismanoglu and J. Amorim, Brazilian Journal of Physics, vol. 39, no. 1, March, 2009. "Characterization of microhollow cathode discharges".

[43] D. D. Hsu and D. B. Graves, J. Phys. D. Appl. Phys., 36, 2898-2907, 2003. "Microhollow cathode discharge stability with flow and reaction",

[44] R. H. Stark and K. H. Schoenbach, Appl. Phys, vol. 48, No. 4, 1999. "Direct current high-pressure glow discharges".

[45] J. Schulze, B. G. Heil, D. Luggenh¨ olscher, T Mussenbrock, R P Brinkmann and U Czarnetzki. J. Phys. D: Appl. Phys. 41 (2008) 042003 (5pp) "Electron beams in asymmetric capacitively coupled radio frequency discharges at low pressures".

[46] S. Okazaki, M. Kogomat, M. Uehara and Y. Kimura. J. phys, D; Appl, Phys, 26 (1993) 889- 892." Appearance of stable glow discharge in air, argon, oxygen and nitrogen at atmospheric pressure using a 50 Hz source".

[47] T. Jiang, Y. Li, C-j Liu, G-h. Xu, B. Eliasson, B. Xue. Elsevier Catalysis today 72 (2002) 229-235."Plasma methane conversion using dielectric-barrier discharges with zeolite A"

[48] K. Thanyachotpaiboon and S. Chavadej, T.A. Caldwell, L.L. Lobban, and R.G. Mallinson, AIChE Journal, October 1998 Vol. 44, No.10."Conversion of Methane to Higher Hydrocarbons in AC Nonequilibrium Plasma"

[49] T. Nozaki, A. Hattori, K. Okazaki, ELSEVIER Catalysis Today 98 (2004) 607-616. "Partial oxidation of methane using a microscale non-equilibrium plasma reactor".

[50] Seung-soo Kim, H. Lee, J. W. Choi, Byung-ki Na, and K. Song. J. Ind. Eng. Chem., Vol.9, No.6, (2003) 787-791."Kinetics of the Methane Decomposition in Dielectric-Barrier Discharge".

[51] C.-J. Liu, B. Eliasson, F.He, Y. Li, G.-H. Xu, Plasma Chem. Plasma Process. 21 (2001) 301.

[52] B. Eliasson, C.-J. Liu, U. Kogelschatz, Ind. Eng. Chem. Res.39 (2000) 1221.

[53] F. He, C.-J. Liu, B. Xue, surface interface Anal. 32 (2001) 198.

[54] S. kado, K. Urasaki, Y. Sekine, K. FuJimoto. Elsevier Fuel 82 (2003) 1377-1385 "Direct conversion of methane to acetylene or syngas at room temperature using Non-equilibrium pulsed discharge".

[55] C-J. Liu, B. Xue, B. Eliasson, F. He, Y. Li, and G-H. Xu. Plasma Chemistry and Plasma Processing,Vol.21,No.3,2001."Methane Conversion to Higher Hydrocarbons in the Presence of carbon dioxide Using Dielectric-Barrier Discharge Plasmas".

[56] S-S. Kim, H. Lee, B-K. Na and H. K. Song.Korean J. Chem. Eng., 20(5), 869-872 (2003). "Reaction Pathways of Methane Conversion in Dielectric-Barrier Discharge."

[57] A. Agıral, C. Trionfetti, L. Lefferts , K. Seshan, J.G.E.(Han) Gardeniers Chem. Eng. Technol. 2008, 31,No.8,1116–1123."Propane Conversion at Ambient Temperatures C–C and C–H bond Activation Using Cold Plasma in a Micro-reactor."

[58] R. M. Tiggelaaretal., Chem. Eng. J. 2007, 131, 163.

[59] B.Eliasson, C.J.Liu, U.Kogelschatz, Ind.Eng.Chem.Res.2000, 39,1221.

[60] F. Ouni, A. Khacef, J. M. Cormier. Plasma Chem Plasma Process(2009)29:119–130 "Syngas Production from Propane Using Atmospheric Non-thermal Plasma."

[61] K. Fouhy, G. Ondrey (1996)ChemEng103:46–47.

[62] D. R. Cohn, A. Rabinovich, C. H. Titus, L. Bromberg (1997) Int J .Hydrogen Energy 22:715-723.

[63] S. Freni, G. Calogero, S. Cavallaro (2000) J. Power Sources86:90–97.

[64] M.A. Pena, J.P. Gomez, L.G. Fierro (1996) J.Appl.CatalA144:7–57.

[65] L.A. Rosocha , Y. Kim , G. K. Anderson , and S. Abbate.
International Journal of Plasma Enviprmental Science & Technology Vol.1 No.1 March 2007. "Combustion Enhancement Using Silent Electrical Discharges".

[66] T. V. Choudary, E. Aksoylu, D. W. Goodman, Catal.Rev.2003, 45(1), 151

[67] B. Eliasson, C.-J. Liu, U. Kogelschatz, Ind.Eng.Chem.Res.39(2000)1221.

[68] C.-J. Liu, R. Mallinson, L.Lobban,Appl.Catal.A178(1999)17.

[69] S. L. Yao, F. Ouyang, A. Nakayama, E. Suzuki, M. Okumoto, A. Mizuno,
Energy Fuels14(2000)910.

70) S. Kado, Y. Sekine, K. Fujimoto, Chem. Commun.(1999) 2485.

[71] H. Matsumoto, S. Tanabe, K. Okitsu, Y. Hayashi, S. L. Suib, J. Phys. Chem.A105 (2001) 5304.

[72] H.-K. Jeong, S.-C. Kim, C. Han, H.Lee, H.K.Song, B.-K. Na, Korean J. Chem. Eng.18(2001) 196.

[73] C.-J. Liu, B. Xue, B.Eliasson, F.He, Y.Li, G.-H. Xu, Plasma. Chem.Plasma Process.21(2001)301.

[74] J. M. Cormier, "Non Equilibrium Plasmas and Chemistry''

[75] K. Pochner, W. Neff, R. Lebert, Surf. & Coat. Tech. 74 – 75, 394 – 398, 1995.108
"Atmospheric pressure gas discharges for surface treatment,"

[76] J. Y. Jeong, S. E. Babayan, A. Schutze, V. J. Tu, J. Park, I. Henins, R. F. Hicks, and G. S. ," J. Vac.Sci. Tech. A, vol.17, pp. 2581-2585, 1999.106
Selwyn, "Etching polyimide with a nonequilibrium atmospheric-pressure plasma jet,"

[77] Y. Sawada, S. Ogawa, and M. Kogoma, J. Phys. D: Appl. Phys., vol 28, pp. 1661-1669, 1995. "Synthesis of plasma-polymerized tetraethoxysilane and hexamethyldisiloxane films prepared by atmospheric pressure glow discharge,"

[78] T. A. Beer, J. Laimer, H. Störi, Surf. Coat. Tech. 120,331 – 336, 1999.
"Dynamics of a pulsed DC discharge used for plasma-assisted chemical vapor deposition: a case study for titanium nitride deposition,"

[79] D. Wang, Y. Wang and C. Liu, Thin Solid Film 506 – 507 (2006) 384 – 388.
"Multi-peak behavior and mode transition of a homogeneous barrier discharge in atmospheric pressure helium,"

[80] V. I. Gibalov, G. J. Pietsch, J. Phys. D: Appl. Phys. 33, 2618 – 2636, 2000.
"The development of dielectric barrier discharges in gas gaps and on surfaces,"

[81] X. Xu, Thin solid Films 390(2001) 237-242.
"Dielectric barrier discharge- properties and application".

[82] L. A. Rosocha, Plasma Physics Group, Los Alamos National Laboratory, 2003.

Appendix A

Permittivity is a physical quantity that describes how an electric field affects, and is affected by, a dielectric medium, and is determined by the ability of a material to polarize in response to the field, and thereby reduce the total electric field inside the material. So, it is defined as material's capability to transfer an electric field. It is directly related to electrical susceptibility.

The permittivity of a material is usually given relative to that of vacuum, as a relative permittivity ε_r, which is commonly called dielectric constant. The actual permittivity ε is then evaluated by multiplying the relative permittivity ε_r by vacuum permittivity ε_o, which is as follows:

$$\varepsilon = \varepsilon_r \varepsilon_{o,}$$

$$K = \varepsilon_r = 9.5$$

$$\varepsilon_o = 1/c^2 * \mu_o \approx 8.8541878176 * 10^{-12} \text{ F/m},$$

where K is dielectric constant or relative permittivity for material, c is the speed of light (299792458 m/s), and μ_o is the vacuum permeability constant ($4\pi \times 10^{-7}$ N/A^2).

Therefore actual dielectric constant for alumina oxide is:

$$\varepsilon = 8.8541878176 * 10^{-12} \text{ F/m} * 9.5 = 84.11 * 10^{-12} \text{ F/m}$$

Capacitance of dielectric discharge is calculated as follows:

$$C = (\varepsilon_r \varepsilon_o A)/d$$

where "A" is the capacitance surface area, and "d"is distance between two electrodes.

$$C = (84.11 * 10^{-12} \text{ F/m} * 0.006325 \text{ m}^2)/(0.003) \text{ (m)} = 177.3319 * 10^{-12} \text{ F}$$

CURRICULUM VITA

Atul Vitthalrao Ambhore was born in Amaravati, Maharastra, India. He enrolled at the Karamvir Dadasaheb Kannamwar (K.D.K.) Engineering College, Nagpur, India in July 1997, where he obtained a Bachelor of Mechanical Engineering in May of 2003. He worked in DCS Company Nagpur as a trainee engineer from May 2004 to May 2005. He later continued his graduate studies in Mechanical Engineering from The University of Texas at El Paso in August of 2005 under the guidance of Dr. Evgeny Shafirovich. He worked as a research and teaching assistant in Mechanical Engineering Department.

Permanent Address: Jay Prakash Nagar plot no.50
Dharampeth 5 th Lay out
Kahamala Nagpur. 440025
Maharashtra, India.

This thesis was typed by Atut V. Ambhore.